ACS PHYSICAL CHEMISTRY Au
AN OPEN ACCESS JOURNAL OF THE AMERICAN CHEMICAL SOCIETY

pubs.acs.org/physchemau

Review

The Rise and Future of Discrete Organic–Inorganic Hybrid Nanomaterials

Matthew W. Brett,[†] Calum K. Gordon,[†] Jake Hardy,[†] and Nathaniel J. L. K. Davis*

Cite This: *ACS Phys. Chem Au* 2022, 2, 364–387

Read Online

ACCESS | Metrics & More | Article Recommendations

ABSTRACT: Hybrid nanomaterials (HNs), the combination of organic semiconductor ligands attached to nanocrystal semiconductor quantum dots, have applications that span a range of practical fields, including biology, chemistry, medical imaging, and optoelectronics. Specifically, HNs operate as discrete, tunable systems that can perform prompt fluorescence, energy transfer, singlet fission, upconversion, and/or thermally activated delayed fluorescence. Interest in HNs has naturally grown over the years due to their tunability and broad spectrum of applications. This Review presents a brief introduction to the components of HNs, before expanding on the characterization and applications of HNs. Finally, the future of HN applications is discussed.

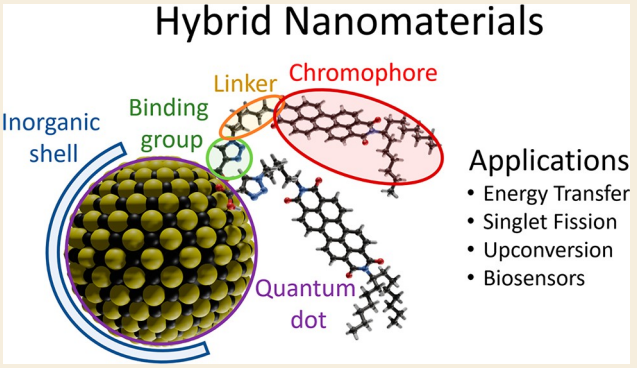

KEYWORDS: *Hybrid Nanomaterials, Energy Transfer, Singlet Fission, Upconversion, Thermally Activated Delayed Fluorescence, Quantum Dot, Chromophore*

1. INTRODUCTION

Recently, there has been an increase in research in the field of organic semiconductor ligands attached to nanocrystals (NCs) (typically quantum dots (QDs)), replacing ligands that offer colloidal stability with ones that add additional optoelectronic properties. For this Review, we define hybrid nanomaterials (HNs) as the combination of an inorganic NC or QD and an attached organic semiconductor/chromophore (ligand), which is usually a conjugated small molecule (Figure 1a). By combining the ease of attachment/functionalization of the organic component with the tunability (via confinement effects[1]) of QDs, HNs present a new and versatile class of optoelectronic materials with properties beyond the sum of the individual components. This versatility has been utilized across different optoelectronic disciplines such as biology,[2−7] chemistry,[8−10] electronics,[11] optics,[12,13] photophysics,[14,15] photovoltaics,[16,17] and spectral management,[10,18−25] and it is the dominant reason for the rapid increase in recent publications (Figure 1b).

While there are recent reviews on both the design of specific ligands for photophysical control[26] and utilizing organic/inorganic interfaces for spectral management,[27] this Review aims to focus on the fabrication of this new class of materials. To produce functional and versatile HNs for a variety of applications, it is necessary to understand the effects each component part has on the HN system. We will assume a basic knowledge of the two major constituents of HNs, the inorganic and organic semiconductors, and take a more in depth look at how the five major components of HNs control the fabrication and application of these materials. The five major component parts are (1) the QD, (2) any inorganic shells on the QD surface, (3) the binding group of the ligand, (4) the spacer separating the organic chromophore center and the QD (linker), and (5) the organic chromophore itself (Figure 1a). To aid comprehension and discussion, we will briefly touch on common measurement techniques used in the field of HNs. Finally, we will comment on the published applications of these materials based on their potential as a new class of optoelectronic materials.

2. QUANTUM DOTS

QDs are small particles of semiconductor materials, and these QDs have shown potential in optoelectronic applications.[28−30] QDs can be considered as an intermediate species between atoms or molecules and bulk material (Figure 2). As the size of semiconducting NCs is reduced, the electronic transitions shift to higher energy, and the oscillator strength is concentrated into just a few transitions.[31,32] This quantum-size effect

Received: March 24, 2022
Revised: May 5, 2022
Accepted: May 6, 2022
Published: May 28, 2022

https://doi.org/10.1021/acsphyschemau.2c00018
ACS Phys. Chem Au 2022, 2, 364–387

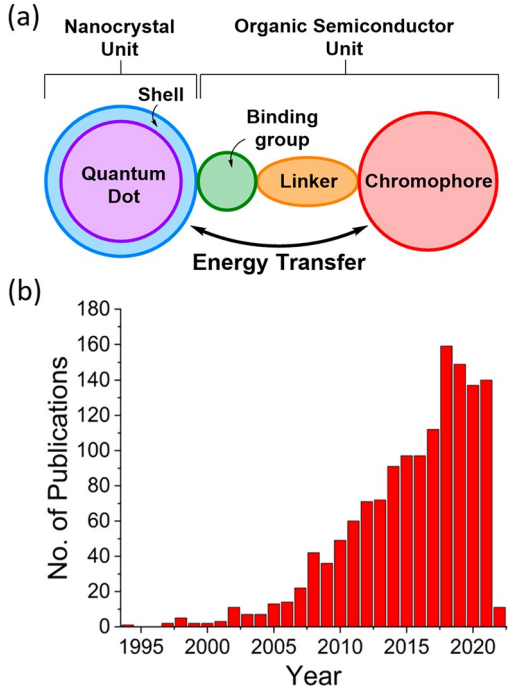

Figure 1. (a) General structure of HNs. (b) Histogram analysis from ISI Web of Science with keywords "inorganic organic hybrid quantum dot".

drastically modifies the energy spectra of three-dimensionally confined NCs.[1] Thus, NC absorption and luminescence are size dependent. QDs energy levels are also dependent on their surface chemistry. Changing binding group type and the dipole moment of a surface ligand changes the strength of the QD-ligand surface dipole, shifting the vacuum energy and, in turn, the QD valence band maximum and conduction band minimum.[33]

Over the past decade, research has focused on optimizing the synthesis of semiconductor NC QDs. Synthetic routes utilizing organometallic precursors enable the production of nanocrystalline particles with near monodisperse size distribution.[35] The preparation of nearly monodisperse well passivated NC samples is essential to permit studies that distinguish the truly novel properties inherent to nanoscale structures from those associated with structural heterogeneities or polydispersity. NC samples must be uniform not only in size and shape, but they must also have well-formed crystalline cores and controlled surface chemistry.[36]

Typically, monodisperse QDs are synthesized by a hot injection method.[37,38] Briefly, the hot injection method entails the rapid injection of a precursor to a hot reaction mixture/solvent. Nuclei are formed immediately upon injection. As the nuclei form, concentration and temperature drop, disabling the formation of any new nuclei. Leftover precursor reagents grow onto existing nuclei, forming monodisperse QDs.

QDs have gained attention due to their large absorption coefficients,[39] which can extend into the NIR,[35,40−45] efficient spin−orbit coupling for the emission of transferred triplet excitons,[26] and improved photostability compared with their organic counterparts.[46,47] In addition, it remains difficult to synthesize organic molecules that absorb and emit strongly at energies below 900 nm. Those that have been made typically undergo rapid internal conversion to the ground state.[48]

As discussed, the energy levels of QDs are dependent on both the QD size and the surface chemistry.[33] While size can be controlled during the QD synthesis, the surface chemistry can be modified either by the growth of an external inorganic shell[49−51] or via subsequent exchange of the colloidally stabilizing ligands.[33]

3. INORGANIC SHELLS

Due to their geometry, QDs have a distinct difference between their surface and bulk crystal lattice chemistry. At the surface of a crystal, the periodicity of the bulk crystal lattice gives way to faceting, bond contraction, reconstruction, unsaturated/dangling bonds as well as physisorbed and chemisorbed molecular species. With dimensions on the order of a few nanometers, many of the atoms in NCs are located at or near the surface.[52] This high surface area to volume ratio makes NCs prone to

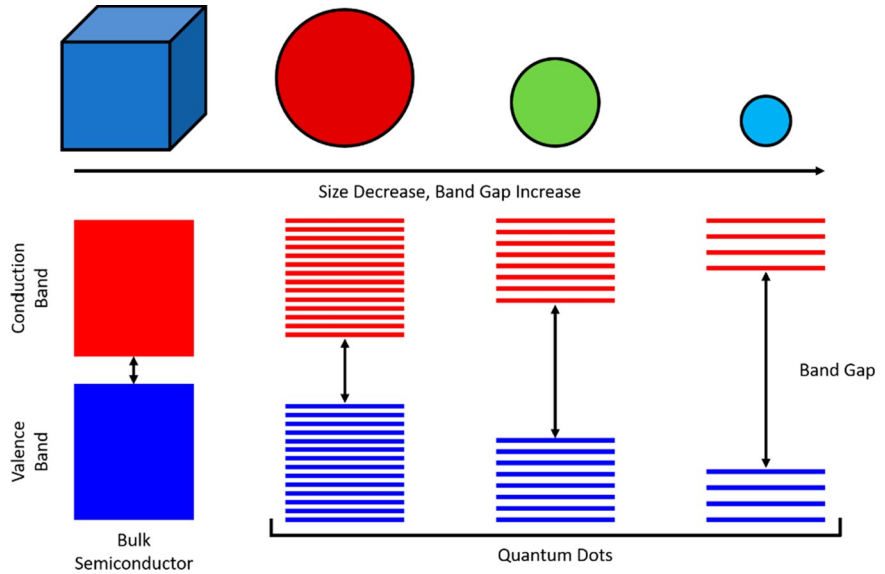

Figure 2. Illustration of quantum confinement effect on the band gap of general semiconductors. Adapted from ref 34. Copyright 2018 with permission from Elsevier.

https://doi.org/10.1021/acsphyschemau.2c00018
ACS Phys. Chem Au 2022, 2, 364−387

Table 1. Examples of Core/Shell QD Structures Used to form HNs

QDs	band gap tunability	shells	application
InP	450−700 nm[64]	ZnSe, ZnS	FRET,[6] upconversion[65]
CdSe	450−650 nm[66]	ZnS, CdS	FRET,[13] upconversion,[22,68,69] thermally activated delayed emission[70]
CdS	390−440 nm[67]		
PbSe	0.6−4 μm[71]	CdS	singlet fission,[20,72,73] triplet energy transfer,[74] upconversion[75−78]
PbS	800−1400 nm[35]		
$CsPbX_3$ (X = Cl, Br or I)	400−690 nm[79]		singlet fission,[18] triplet energy transfer,[80] upconversion,[23,81] thermally activated delayed emission[82]
$CuInS_2$	450−900 nm[83]	ZnS	FRET,[84] upconversion[85]
Si	355−1130 nm[86]		energy transfer,[12] upconversion[87]
$NaYbF_4:Tm^{3+}$	∼40, ∼360, ∼450, ∼475, ∼510, ∼580, ∼650 nm[88]	$NaYF_4:Nd^{3+}$	energy transfer cascade,[88] upconversion[88]

high trap state densities. Imperfectly passivated surfaces promote nonradiative recombination of charge carriers and are detrimental to optical and device performance.[53,54] To improve QDs optical properties, chemical stability, and photostability, several approaches have been developed, including passivation of the NC surfaces with inorganic shells.[43,55] These inorganic shells are limited to having the same crystal structure as the QD core and must have minimal lattice mismatch for adequate passivation. Examples of core/shell QD structures are listed in Table 1.

Several commonly used methods exist for the formation of shells: Successive ionic layer adsorption and reaction (SILAR),[56−59] in which cationic and anionic precursors are added separately to form monolayers one at a time (Figure 3).

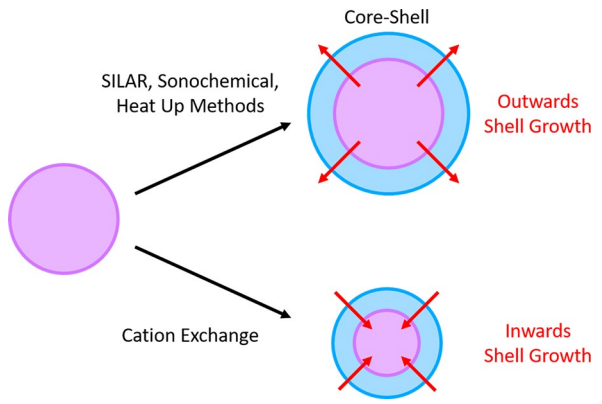

Figure 3. Different methods of inorganic shell growth onto core QDs.

Cation exchange, in which introduced precursor cations exchange with cations within the core QD, causing an inward growth of a shell (Figure 3). Sonochemical,[60,61] where sonication induces a reaction between precursors forming a shell. Finally, heat up methods, where precursors are added and gradually heated to a desired reaction temperature, are also used.[62,63] While these measures have achieved varying levels of success, they result in complex, heterostructured materials with altered carrier dynamics.[43]

Another technique is to replace the long insulating ligands that enable colloidal stability following synthesis with short organic linkers, potentially leading to improved surface coverage and higher packing densities.[54,89,90] Attached ligands can positively and negatively influence carrier mobility,[91−93] tunneling distance,[94,95] dielectric environment,[96,97] carrier and exciton lifetimes,[98−101] electronic trap sites,[96,99−101] surface dipoles,[33] and valence and conduction band edges.[33] However, this Review aims to focus on the relatively new idea of replacing these colloidally stabilizing ligands with ligands that offer new optical and electronic functionality. In general, a chromophore ligand can be broken into three parts: the binding group, the linker, and the chromophore.

4. BINDING GROUPS

As mentioned above, the surface atoms of a QD have lower coordination than the core atoms, resulting in free sites with unbonded orbitals.[102] These unbonded orbitals allow for interaction with ligands, which can increase passivation of surface traps[103] and help prevent aggregation of the QD.[102,104] The portion of the ligand interacting with the surface orbitals of the QD is called the ligand binding group. In the simplest form, binding to the QD surface involves the transfer or exchange of electrons between a surface atom and the ligand binding group.[105] The Covalent Bond Classification has been used to describe these surface interactions, with ligands defined as either L-, X-, or Z-type based on the number of electrons contributed to the surface bond from the neutral ligand (2, 1, or 0 respectively, Figure 4).[105]

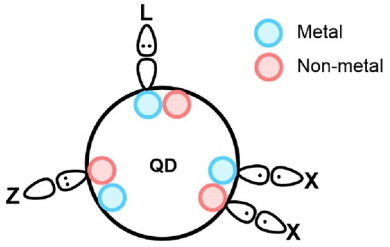

Figure 4. Representation of the three ligand classes used to describe nanoparticle ligands. L-, X-, and Z-type ligands donate 2, 1, and 0 electrons to the QD surface, respectively.[105]

A wide range of ligand binding groups have been used to efficiently bind to different QD crystal structures (Figure 5).[106] The simplest method of attaching a ligand to a nanoparticle is through physisorption, whereby van der Waals forces facilitate a weak binding between the ligand and QD surface.[107−109] Monodentate ligands can also be used to attach ligands to the QD surface, for example, with carboxylic acids,[8−10,106,110,111] amines,[106,111−114] thiols,[106,111,115−117] or phosphorus based binding groups.[106,111,118,119] These binding groups connect the QDs and ligands with chemisorption,[111] thus providing a stronger interaction than the physisorption method. Multidentate ligands have multiple binding groups on a single ligand, allowing the chelate effect to provide ligands with more stability on the QD surface, reducing ligand desorption.[120]

https://doi.org/10.1021/acsphyschemau.2c00018
ACS Phys. Chem Au 2022, 2, 364−387

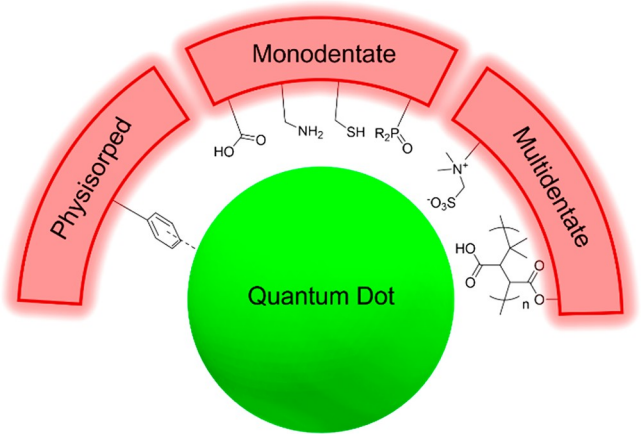

Figure 5. Examples of linkers that have can be used to bind a chromophore to QD.[8−10,106−125]

Multidentate ligand binding groups include zwitterions[121−123] and polymers.[123−125]

Binding strength is arguably the most important consideration for a hybrid system: without adequate binding, the ligand will not remain attached. As such, in selecting a binding group for a hybrid organic−inorganic system, the aim should be to maximize ligand binding strength without negatively influencing the desired properties of the system. Optimizing the binding group to meet these two aims for each hybrid system is often a balancing act. There is a range of factors that may need to be considered when selecting a binding group including (but not limited to): (1) composition of the QD;[105,121] () postsynthetic treatment method of the hybrid QDs; (3) application requirements for the HN; (4) steric effects of the organic ligand; (5) desired ligand density; and (6) ease of access to the desired binding group.

Of these factors, several directly affect the binding strength required. The composition of the QD influences the interactions between QD and ligand and can result in facile ligand desorption if binding is inadequate. An example of this is in the functionalization of $CsPbBr_3$ perovskite QDs, where it has been found that monodentate ligands have dynamic surface interactions resulting in poor QD stability over time.[105,121] To overcome this, a range of bidentate zwitterionic ligands have been employed, using the chelate effect to reduce the effects of the dynamic nature of the $CsPbBr_3$ QDs.[121] Vigorous centrifugation and solvation are used in the postsynthetic purification of the QDs, which can cause ligand dissociation with weak binding. Similarly, ligand dissociation is more prevalent in solution than solid state, so the final application of the particles also needs to be considered in selecting the binding group. While considerations of the medium containing a HN is beyond the scope of this review, it is important to note that the dielectric constant of the immediate solvent environment affects the charge distribution of the NC,[126] and the organic component,[127] influencing binding strength. Finally, the steric bulk of the ligand near to the QD may reduce the efficacy of the binding group, requiring stronger binding groups.

Binding strength aside, it is important to consider the desired ligand density for a HN. The more space that the binding group requires on the surface of the QD, the fewer ligands that can fit on the surface. In cases where ligand density needs to be sufficiently high, it can be useful to select monodentate binding groups over the stronger binding multidentate groups. Finally, the design of an organic ligand with a particular binding group will often not be commercially available and thus may require in-house synthesis to be made. Depending on the sensitivity of the system, it is often worthwhile selecting more accessible binding groups that do not require significant synthetic work. Selecting a binding group that balances all factors to provide a solution suitable for the application is often a challenge that requires testing and optimization to achieve.

5. LINKER

The linker section of the HN system acts to connect the binding group to the chromophore. While it is not essential to the HN system, it can improve the overall function.[26] As the field of HNs is intrinsically dependent on the energy transfer between NC and ligand, the distance between the two components plays an important role. The linker can be used to effectively tune the distance (and thus the energy transfer occurring) in the HN system.[24−26,128,129] The linker also acts to spatially separate the binding group and chromophore, reducing negative influences (typically electronic or steric) that can arise from directly connecting the binding group to the chromophore.

Linkers do not have any specific structural requirements, although they tend to be chemically, electronically, and optically inert to avoid unwanted interactions with the HN system. Literature examples of linkers have not had much diversity, likely due to the synthetic requirement for designing a diverse linker. Common linkers tend to be based on alkyl chains[7,9,26,129,130] or phenyl spacers,[25,26,128,129] sometimes with other structural motifs present due to the synthetic route used, such as triazole rings,[9] ethers[129] or amides[7] (Figure 6).

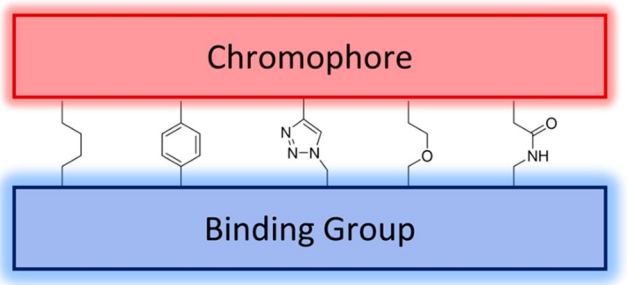

Figure 6. Examples of linkers that can be used to connect chromophores to binding groups.[7,9,25,26,128−130] Note that these exact structures may not have necessarily been used, only the functionality.

The fact that linkers are not essential to the function of a HN system and tend to require organic synthesis to include, often results in their exclusion from this system.[10,18,22,23,75] Despite this, some situations require a linker to distance the chromophore from the nanoparticle surface. For example, Xu et al. designed a HN system that worked as an energy transfer cascade, from QD to surface chromophore to solution chromophore (Figure 7).[25] With increasing linker length, the efficiency of the first energy transfer decreased but the efficiency of the second energy transfer increased.[25] Thus, the linker length was used to optimize the efficiency of the entire process.[25] Thus, it is a necessary step to consider whether a linker in required for the specific application.

https://doi.org/10.1021/acsphyschemau.2c00018
ACS Phys. Chem Au 2022, 2, 364−387

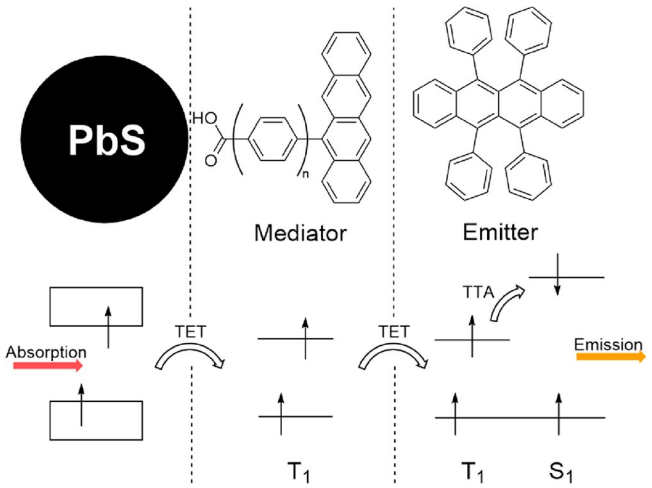

Figure 7. Energy transfer cascade from a PbS NC to a rubrene emitter, via a mediator tetracene with variable distance from the crystal. The energy transfer efficiency optimized through the length of the linker system used, by changing the number of phenyl rings (n). Adapted from ref 25. Copyright 2020 American Chemical Society.

If decided that a linker would be beneficial for a particular HN system, there is a range of factors that should be considered in selecting a linker including: (1) the desired length of the linker; (2) the flexibility and sterics of the linker; (3) the electronics of the linker; and (4) the accessibility of the linker. As the inclusion of a linker is typically synthetically demanding, investigations into these factors are currently limited.[26] Instead, we will discuss the broader reasoning behind these considerations, providing literature examples where available.

Primarily, a linker acts to provide distance between the QD and chromophore. The power of the linker length comes in the ability to tune this distance to optimize the desired properties of the HN system. However, this makes selecting a linker length for a particular application a challenging task because it depends on many factors specific to each system. For example, a key influence in the choice of linker length is the type of energy transfer expected to take place; for example, Dexter energy transfer requires shorter distances than Förster resonance energy transfer (FRET) does.[131] Linker flexibility and sterics are important factors that needs to be considered in designing a HN system. A flexible linker may allow for chromophores to vary the distance to the QD, altering the energy transfer properties.[132] In addition, flexibility in the linker may reduce the number of chromophores that can fit on the surface of the particle, likely the result of random chromophore movement increasing the disorder of the system, thus increasing the entropic cost of binding.[133] Similarly, if the linker has steric bulk associated with it, it may reduce the quantity of chromophores that can fit around the QD compared to a less bulky linker. In addition, the electronics of the linker can play a part and may need to be considered. For example, if a chromophore is aromatic, then attaching a phenyl linker system can extend the conjugation of the system, influencing the desired properties. In some cases, this extended conjugation may be desired when transmission through the linker is necessary.[25] In addition, the electronics can influence the packing of molecules on the surface. This can either cause unexpected effects such as aggregation induced excimer formation[73] or be desired for other applications like singlet fission.[10] These electronic effects tend to be minimal so linkers with strong electronic influences (such as phenyl rings) are still used.[25]

Depending on the HN system, it is often more sensible to select a linker than can easily be accessed through known synthetic methods. Overall, the selection of a linker involves balancing a range of factors to help optimize the overall function of the HN system.

6. CHROMOPHORES

A chromophore is defined as the part of a molecule in which electronic transitions occur in the visible region and is thus responsible for the color of the molecule.[134] For the purposes of a HN system, chromophores need not necessarily have their transitions in the visible region, so long as the energy is appropriately matched to the QD of choice. Despite this, chromophores used in HN systems tend to fall in the visible region.[6,8−10,18,19,22,23,75,130,135]

The primary selection criteria for choosing a chromophore are the intrinsic properties associated with it. These properties generally include absorption maxima, molar absorptivity, emission maximum, photoluminescent quantum efficiency (PLQE), or Stokes shift.[136] In addition to these innate properties, sometimes the energy levels of the chromophore allow for other processes such as singlet fission (SF) or triplet−triplet annihilation (TTA) to occur (these processes will be discussed in detail later).[10,22,23,75,130] Besides these processes, the selection of a particular chromophore is usually dependent on the energy levels of absorption and/or emission. Energy transfer is an essential process for HN systems; thus, absorption/emission matching is crucial for optimizing this process.[137]

Besides optimizing energy transfer, the selected chromophore needs to have the ability to bind to a QD. Some chromophores innately contain binding groups that can be utilized, such as the carboxylic acid on some rhodamine-based dyes.[6] However, if this is not the case, there needs to be a way to modify the chromophore without negatively impacting the properties. Typically, this simply involves the attachment of an additional handle in place of a hydrogen atom−for example, a single aromatic proton in tetracene can be replaced with a binding group or linker binding group to allow the chromophore's attachment.[10,130] Despite this, most chromophores have portions that can be functionalized with a binding group with only minor effects to the intrinsic properties of the chromophore.

7. METHODS OF CHARACTERIZATION

Hybrid systems as currently described exhibit a multitude of different properties. In many circumstances, one hybrid system cannot be characterized in the same means as another. In this section, we discuss available characterization techniques to cover a wide variety of hybrid systems.

7.1. Förster Resonance Energy Transfer

FRET (Figure 8) is the most extensively researched phenomenon in hybrid systems to date (Table 2).[3,6,7,12,13,138−164] It is also a technique for supporting the findings of whether a donor and acceptor are closely bound.

FRET is a nonradiative energy transfer process occurring from the dipole−dipole coupling of an excited state donor to a ground state acceptor. It is generally only possible from donor−acceptor distances of 1−10 nm. At distances shorter

https://doi.org/10.1021/acsphyschemau.2c00018
ACS Phys. Chem Au 2022, 2, 364−387

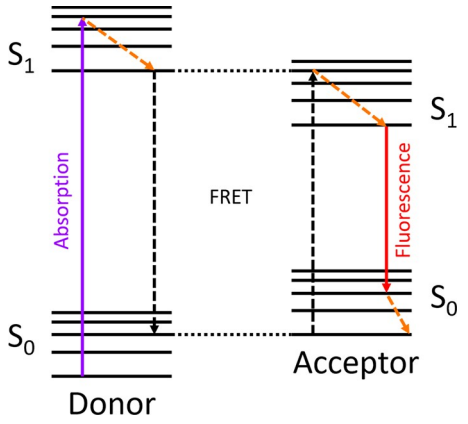

Figure 8. Illustration of FRET, where an excited donor species nonradiatively relaxes by exciting a nearby (1−10 nm) acceptor species.

Table 2. Tabulation of the Commonly Utilized Annihilators for TTA Based Upconversion Systems

annihilator	T_1 (eV)	S_1 (eV)	peak PL (nm)	PLQE (%)
2,5-diphenyloxazole[203]	2.37	3.70	355	95
2,5-diphenyl-1,3,4-oxadiazole[22]	2.82	4.00	443	98
naphthalene[22]	2.72	4.29	320	25
p-terphenyl[22]	2.53	3.92	337	100
9,10-diphenyl anthracene[204]	1.77	3.54	405	100
rubrene[205]	1.14	2.23	557, 591	∼65
5,11-bis(triethylsilylethylnyl)-anthradithiophene[78]	1.08	2.16	580, 610, 660	∼74

than this threshold, Dexter energy transfer typically takes place instead. FRET is described by the following equations:[4,5,165]

$$J(\lambda) = \int F_D(\lambda)\, \varepsilon_A(\lambda)\lambda^4\, d\lambda \tag{1}$$

$$R_0{}^6 = \frac{2.07}{128\pi N_A}\frac{\kappa^2 Q_D}{n^4}J(\lambda) \tag{2}$$

where $J(\lambda)$ is the spectral overlap between the donor emission and acceptor absorption spectrum, R_0 is the distance at which energy transfer between the donor and acceptor is 50%, N_A is the Avogadro constant, κ is the dipole orientation factor, n is the refractive index of the medium, Q_D is the PLQE of the donor in the absence of acceptor, F_D is the emission spectrum of the donor, ε_A is the extinction spectrum of the acceptor, and λ is the wavelength.

$$E = \frac{1}{1 + (r/R_0)^6} \tag{3}$$

where E is the efficiency of energy transfer between donor and acceptor and r is the distance between the donor and acceptor.

Energy transfer efficiencies are commonly characterized by the quenching of the donor species in the presence of acceptor, as shown in eqs 4 and 5.[4,5,165]

$$E = 1 - \frac{F}{F_0} \tag{4}$$

$$E = 1 - \frac{\tau}{\tau_0} \tag{5}$$

where F refers to fluorescent intensity of the donor, τ refers to the lifetime of the donor, and 0 indicates donor with no acceptor present. Using eqs 1−5 allows one to solve the donor−acceptor distance of a given system and hence infer whether ligand binding is likely taking place.

7.2. Dexter Energy Transfer

Similar to FRET, Dexter energy transfer is another short-range energy transfer process that can occur when chromophores are located close to a QD. The Dexter energy transfer process involves the correlated transfer of two electrons between the donor and acceptor (Figure 9).[135,166,167] This transfer requires

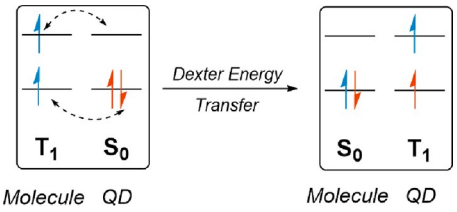

Figure 9. Demonstration of the correlated electron transfer that occurs in Dexter energy transfer from donor (here a molecule in the triplet excited state) to acceptor (here a QD).

short-range correlation (typically <1 nm) to provide adequate orbital overlap between the donor and acceptor.[168] Dexter energy transfer allows triplet energy transfer, a useful property for SF and TTA.[10]

7.3. Stern−Volmer

The Stern−Volmer equation (eq 8)[169] is a powerful tool when characterizing physisorbed hybrid donor−acceptor systems. By collecting both fluorescence and lifetime quenching data as a function of acceptor concentration, the static and dynamic quenching contributions can be established:

$$\frac{F_0}{F} = 1 + K_S[Q] \tag{6}$$

$$\frac{\tau_0}{\tau} = 1 + K_D[Q] \tag{7}$$

$$K = k_q\tau_0 \tag{8}$$

where K_S is the static quenching constant, K_D is the collisional or dynamic quenching constant, Q is the concentration of quencher, K is the Stern−Volmer quenching constant and k_q is the bimolecular quenching constant.

The most important constant for inferring if some form of binding is taking place between a donor and acceptor is k_q, which can be calculated by substituting K for K_S or K_D. If k_q is larger than 1×10^{10} M^{-1}, then some type of binding interaction is taking place[169] (lower than this value indicates poor quenching or steric shielding occurring between the donor and acceptor).

7.4. Changes in Optical Properties and Photoluminescent Properties

Convincing evidence of strong binding between a donor and acceptor is commonly seen when comparing the absorption spectrum of the acceptor to the absorption spectrum of the hybrid system. The acceptor will commonly be red-shifted by 5−15 nm (ref 6.) and the extinction coefficient of the acceptor in some cases has been shown to change.[7,12] This is due to native ligands attached to the donor NC's surface forming an

https://doi.org/10.1021/acsphyschemau.2c00018
ACS Phys. Chem Au 2022, 2, 364−387

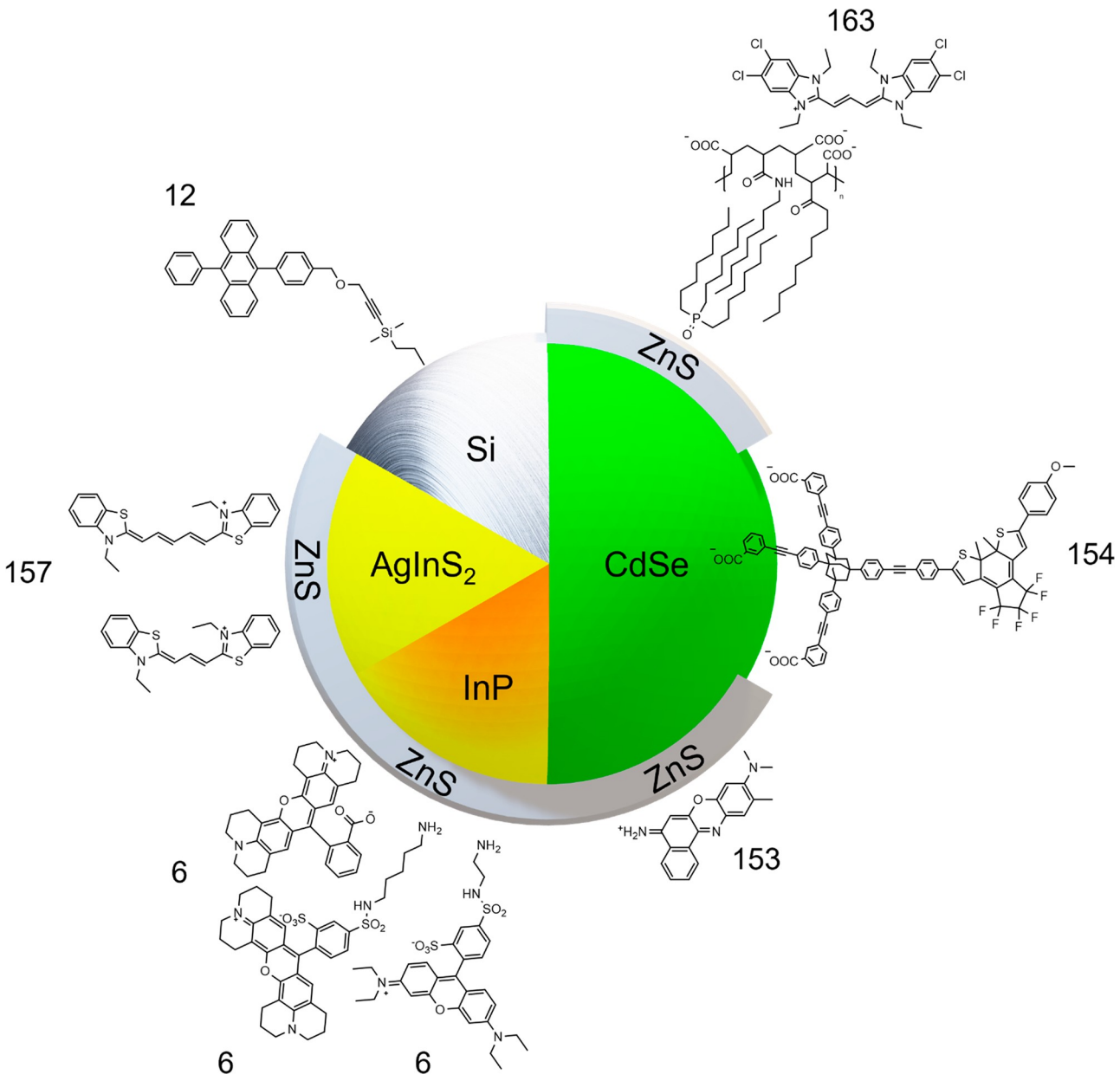

Figure 10. Visual summary of the HNs utilized in FRET based energy transfer systems for nonbiological systems. References of presented research are displayed as numbers around the image.

environment of differing polarity compared to the bulk solvent in which they are dispersed. When an acceptor is bound to the NC surface, the change in the surrounding environments polarity causes these photophysical changes. QDs may also assist the formation of dye aggregates when bound,[170] causing changes to the optical properties of the dye.[171−174]

Evidence of energy transfer can be observed when comparing the excitation spectra of individual donor and acceptor to the excitation spectrum of the acceptor in a hybrid system at the wavelength of the acceptors PL maximum. If energy transfer is present, the hybrid system will exhibit donor excitation character. While this does not directly suggest any form of binding between a donor and acceptor it serves as supporting evidence of an interaction.

In many cases, binding between a donor and acceptor will modify the PLQE of the system.[12] Donor QDs may exhibit a change in PLQE due to bound acceptors changing its passivation at the surface. Acceptors may exhibit a change in PLQE as a function of energy transfer or through the formation of aggregates on the surface.[73]

7.4.1. Ligand Exchange. Observable color and phase changes are a common means of characterizing binding between a donor and acceptor.[7] In any ligand exchange, if sufficient washing is performed post ligand exchange and the color of the clean donor sample is observably different to the exchanged sample (with the absorption spectrum showing acceptor character also present), binding is likely. In a biphasic exchange, if the donor QDs become dispersed in the antisolvent containing the desired ligand to be exchanged, binding is proven.

7.5. NMR

Nuclear magnetic resonance (NMR) spectroscopy is a powerful tool that can be used for the visualization of molecules. For a HN system, it can be used to aid confirmation

https://doi.org/10.1021/acsphyschemau.2c00018
ACS Phys. Chem Au 2022, 2, 364−387

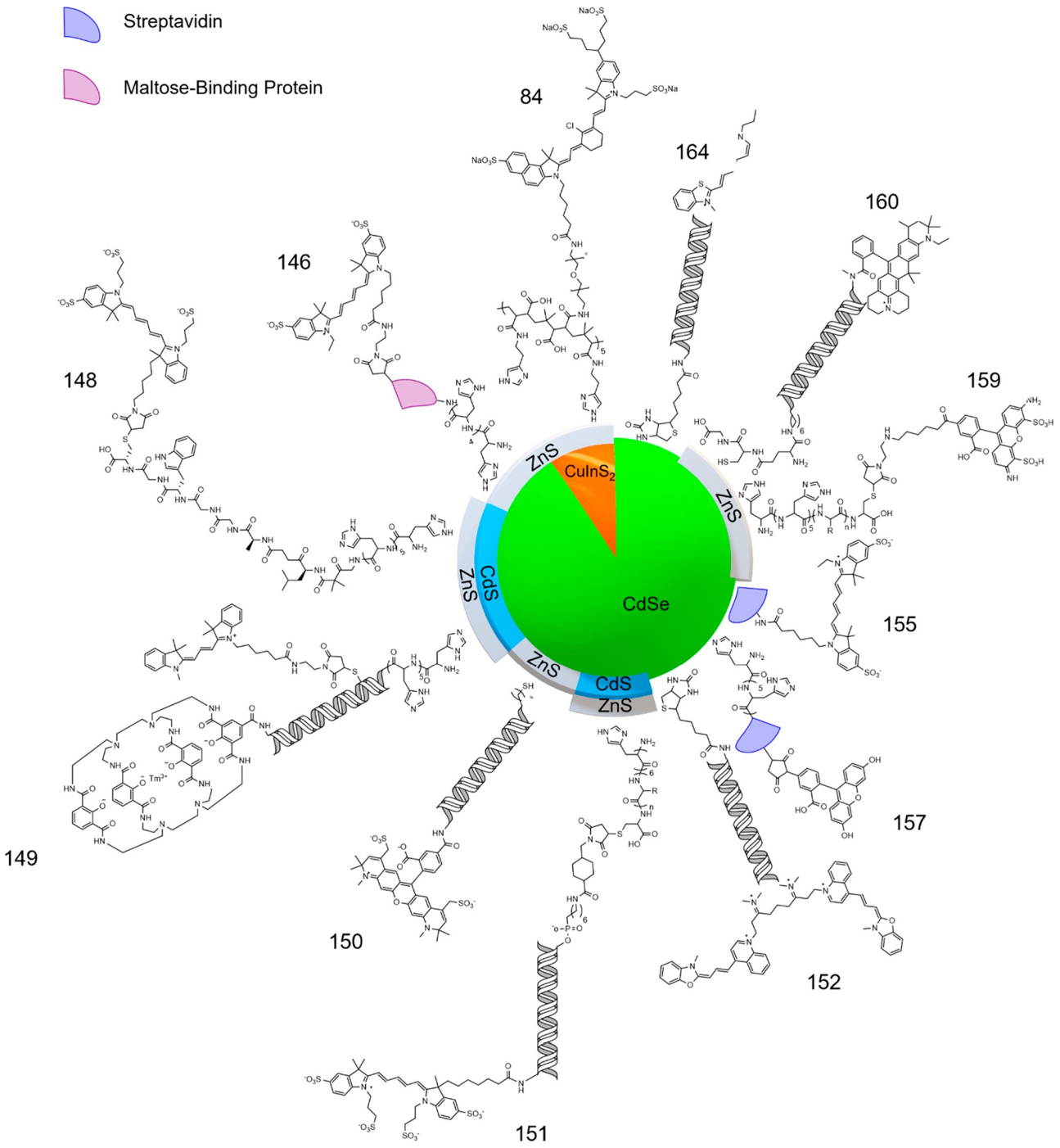

Figure 11. Visual summary of the HNs utilized in FRET based energy transfer systems for biological systems. References of presented research are displayed as numbers around the image.

of chromophore attachment to the surface of a QD.[175] There are several NMR techniques that are used, including one-dimensional (1D) NMR or two-dimensional (2D) diffusion-ordered NMR spectroscopy (DOSY) and nuclear Overhauser effect spectroscopy (NOESY).[175]

1D NMR probes a single spin-active nucleus, for example, ^{1}H, ^{13}C or ^{31}P, to name a few. The 1D NMR spectrum of a molecule is often affected when it is bound to a QD compared to the molecule in solution alone. First, changes in the chemical shift of nuclei in the molecule can indicate binding to a QD,[175] the result of the QD influencing the chemical environment of the molecule. In addition, a broadening of peaks can be observed, a result of attachment to a large QD which tumbles far slower in solution.[121,175] Broadening tends to occur more in atoms closer to the surface of the particle.[175]

Although 1D NMR can give an idea of ligand binding, it is not conclusive. Diffusion-ordered NMR spectroscopy (DOSY), however, can provide this information. DOSY is a 2D NMR technique that measures the diffusion coefficient, *D*, against chemical shift. The diffusion coefficient of the ligand in the QD solution can then be compared to free ligand and should diffuse slower (i.e., lower diffusion coefficient) if bound and attached to a relatively heavy QD.[175] The diffusion

https://doi.org/10.1021/acsphyschemau.2c00018
ACS Phys. Chem Au 2022, 2, 364−387

coefficient, D, can be used in the Stokes−Einstein relation to determine the hydrodynamic diameter, d_H:[175]

$$d_H = \frac{k_B T}{3\pi\eta D} \quad (9)$$

where k_B is the Boltzmann constant, T is the temperature, and η is the solvent viscosity. If the calculated hydrodynamic diameter is roughly equivalent to the sum of the nanoparticle diameter and twice the ligand shell thickness, then the ligand can be assumed to be bound.[175] However, specific note of solvent effects should be considered when determining the hydrodynamic diameter as these have a known effect on ligand conformation.[176−179]

Nuclear Overhauser effect NMR spectroscopy (NOESY) is another technique that can provide more conclusive evidence that a ligand has been bound to the surface of a QD. The nuclear Overhauser effect (NOE) is a distance dependent $^1H-^1H$ internuclear effect, with a 2D NOESY reflecting these interactions and the intensity of the NOE.[175] The sign of a NOE signal depends on the rotational correlation time, τ_c, of the molecule, with relatively long τ_c values giving negative signals and short τ_c's yielding positive signals. When a molecule is attached to a large QD, its rotation is slowed, increasing τ_c and thus affording a negative NOE signal. In comparison, free molecules have short τ_c values, so are observed as a positive signal in the NOE spectrum.[175] This allows for differentiation of bound and unbound molecules.[175]

8. APPLICATIONS

8.1. Energy Transfer

HNs have been used extensively in the development of FRET Based Systems (Figures 10 and 11).

FRET is a powerful tool in potential medical imaging applications, resulting in a collection of well researched hybrid systems (Figure 10).[6,7,142−164] Thomas et al.[6] (Figure 12) first

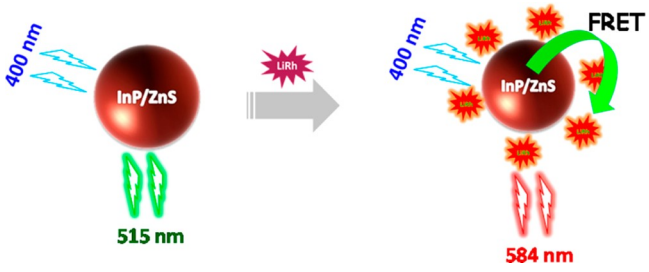

Figure 12. FRET occurring from InP/ZnS to lissamine rhodamine B-ethylenediamine. Adapted from ref 6. Copyright 2014 American Chemical Society.

showed that FRET was possible from (Cd/Pb free) InP/ZnS QDs to emissive organic acceptors. The authors synthesized InP QDs by hot injection. As as-synthesized InP QDs without further treatment exhibit <1% PLQEs,[180] the authors overcoated a ZnS shell by a heat up method, yielding core/shell QDs with a PLQE of ≈10%. Acceptor molecules were chosen to maximize FRET, and this included lissamine rhodamine B-ethylenediamine (LiRh), Texas red cadaverine C5 (TxRed), and rhodamine 101 (Rh101). Each organic dye exhibited good spectral overlap, required for FRET, carboxylate or amine binding groups for attachment to the QDs, and small linker lengths to minimize donor−acceptor distance. Attachment of the acceptors was performed by a Stern−Volmer quenching experiment, in which the authors found a high bimolecular constants (1.71×10^{14} M^{-1} s^{-1} for LiRh, 2.28×10^{14} M^{-1} s^{-1} for TxRed, and 6.80×10^{13} M^{-1} s^{-1} Rh101), indicating a static interaction between the donor and acceptors. High levels of energy transfer were determined by fluorescence and lifetime quenching of the donor (≈60% for LiRh, ≈72% for TxRed, and ≈74% Rh101).

Xia et al.[7] assembled a FRET pair between colloidal $CuInS_2$/ZnS QDs and a dark quencher (Figure 13), for biological

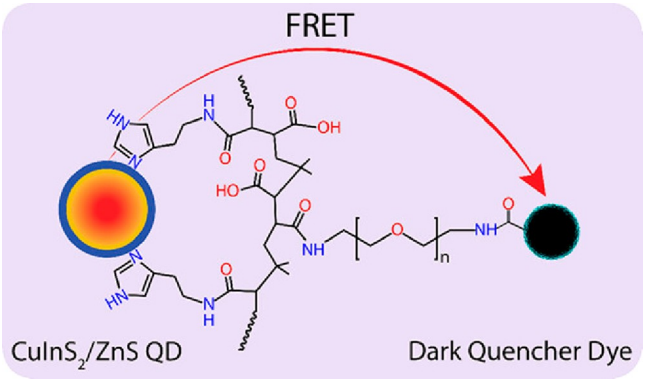

Figure 13. FRET occurring from $CuInS_2$/ZnS to IRDye QC-1. Adapted from ref 7. Copyright 2020 American Chemical Society.

applications such as biomedical imaging, photodynamic therapy, and diagnostic and sensing devices. The work performed by Xia et al.[7] is a particularly good example of the power that tunable hybrid systems have to offer, as they carefully choose each component of their hybrid system to fit their desired purpose. The authors synthesized $CuInS_2$ cores NCs by a heat up method. The cores were chosen for their reduced toxicity compared to cadmium-based alternatives.[181−185] Similar to the work by Thomas et al.,[6] a thin ZnS shell was then overcoated through a SILAR method, with the resultant passivation increasing the core QD PLQEs from ≈20 to ≈50%. While FRET is readily achievable using the cores alone, a donor with a high PLQE is desirable to improve sensitivity when in the presence of the dark quencher. As a foundation for quencher attachment, and to allow for water solubility of the synthesized dots, the authors synthesized two polymer ligands, whose monomers consisted of an imidazole ring for binding, methoxy termination (His-PIMA-PEG-OMe) for one polymer ligand, and amine termination (His-PIMA-PEG-NH_2) for the other. Native oleate ligands on $CuInS_2$/ZnS were exchanged for the polymer ligands, forming two separate dispersions of polymer functionalized $CuInS_2$/ZnS QDs in water. The difference in terminal functionalization allowed for the comparison of binding strength to quencher (IRDye QC-1). The OMe functionalized $CuInS_2$/ZnS QDs showed a small quenching effect in the presence of the quencher, whereas in contrast, using NHS ester reaction chemistry the quencher was covalently bound to the amine functionalized $CuInS_2$/ZnS QDs. The quenching effect was prominent, and the estimated FRET efficiency of their system reaches nearly ≈80% (estimated by lifetime quenching of the donor). The work performed illustrates a clear, comparable example in which a covalently attached donor−acceptor HN within a given medium outperforms (in terms of FRET) the individual,

https://doi.org/10.1021/acsphyschemau.2c00018
ACS Phys. Chem Au 2022, 2, 364−387

unattached donor and acceptor of the aforementioned HN, within the same medium.

The use of hybrid systems is not limited to medical applications, and recent research has explored their use in improving existing solar technologies.[12,13] Tummeltshammer et al.[13] explored the usage of a hybrid system for the use of luminescent solar concentrators (LSCs) by the fabrication of the first proof-of-concept HN LSC (Figure 14). The theory

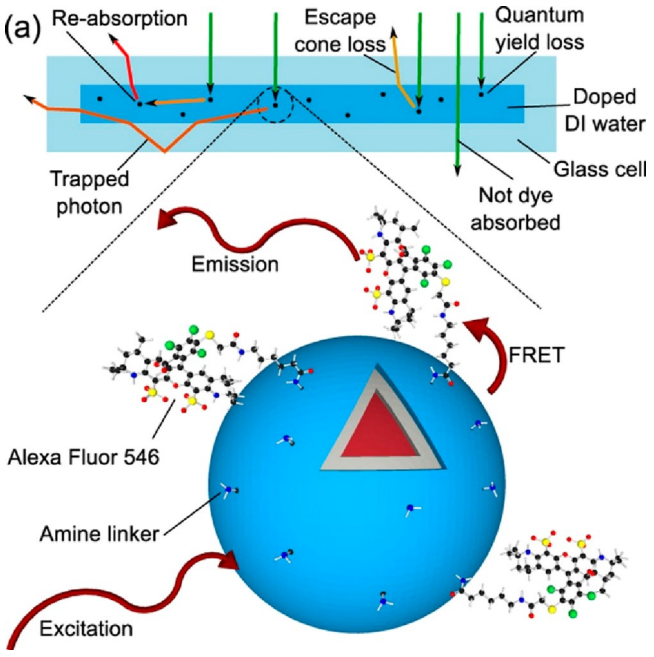

Figure 14. HN system for use in a liquid LSC. Reprinted with permission under a Creative Commons Attribution 4.0 International License from ref 13. Copyright 2017 Elsevier.

being that reabsorption by the high extinction coefficient QDs can be reduced if absorbed energy is transferred to an organic luminophore whose emission spectrum has reduced overlap with the donor's absorption spectrum. CdSe based QDs (Qdot 545 ITK amino (PEG)) were used as the donor. Alexa Fluor 546 NHS ester dye was chosen as an acceptor for its suitable spectral overlap and readily reactive ester to allow for attachment by NHS ester reaction chemistry to the amphiphilic surface coating of the donor. The resultant hybrid system was dispersed in deionized water, and the FRET efficiency was estimated as ≈94% by lifetime quenching of the donor. The hybrid dispersion was then injected into a 2 cm × 2 cm glass cell, forming a liquid-based LSC. Optical efficiency (η_{opt}, defined below) was obtained from AM1.5 g illumination.

$$\eta_{opt} = \frac{PL_{LSC}}{PL_{EXCT} \times G} \tag{10}$$

where PL_{LSC} is the photoluminescent intensity of the edges of a LSC, PL_{EXCT} is the photoluminescent intensity of the excitation source, and G is the size factor (calculated as the ratio between the surface of the top slab compared to the edges of the LSC). An η_{opt} of 2.87% was measured for the hybrid system, in contrast to 2.11% and 2.24% for the Alexa Fluor dye and QDs, respectively. While this work does not particularly contribute to new knowledge of hybrid systems, it does importantly show a new step in terms of versatility of application, being the first published work exploring hybrid systems for use in LSCs.

Mazzaro et al.[12] explored the first hybrid luminophore based solid state LSCs. Silicon NCs (SiNCs) were chosen as the primary luminophore for the authors LSCs, due to their inherently low reabsorption. SiNCs by themselves however offer poor sensitization of the solar spectrum; thus, the authors sought to form hybrid SiNCs functionalized with 9,10-diphenylanthracene (DPA) as a UV sensitizer. SiNCs were produced by thermal disproportionation of hydrogen silsequioxane, obtaining SiNCs in SiO_2. Etching the oxide matrix with HF yields free-standing H-terminated SiNCs. Hydrosilylation with a linker containing an electrophilic site, followed by a substitution reaction with alkyne functionalized 9,10-diphenylanthracene, formed the overall hybrid system. As a control, the authors compared an LSC composed of unbound SiNCs and DPA, which yielded an η_{opt} of 4.25%. In comparison, the LSC composed of the covalently bound counterpart yielded a reduced η_{opt} of 3.08%. This decrease in efficiency was attributed to the hybrid luminophore systems PLQE being decreased in the covalently bound system (PLQE SiNCs 43%, SiNCs with unbound DPA 45%, and SiNCs bound DPA 27%). The authors attribute this decrease to be from the Si core upon covalent functionalization due to decreased ligand passivation, resulting in increased surface defects. Importantly, this paper illustrates the care that must be taken when designing a hybrid system for a given application, as extensive work to ensure the binding of an organic luminophore may not be necessary, and even detrimental, to the desired application.

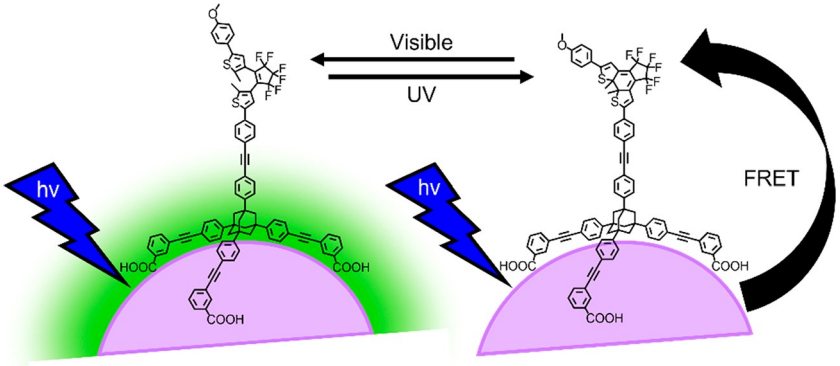

Figure 15. Photochromatic HN system. FRET is the reported photochromic FRET. Adapted with permission under a Creative Commons Attribution 3.0 Unported License from ref 154. Copyright 2014 Royal Society of Chemistry.

https://doi.org/10.1021/acsphyschemau.2c00018
ACS Phys. Chem Au 2022, 2, 364−387

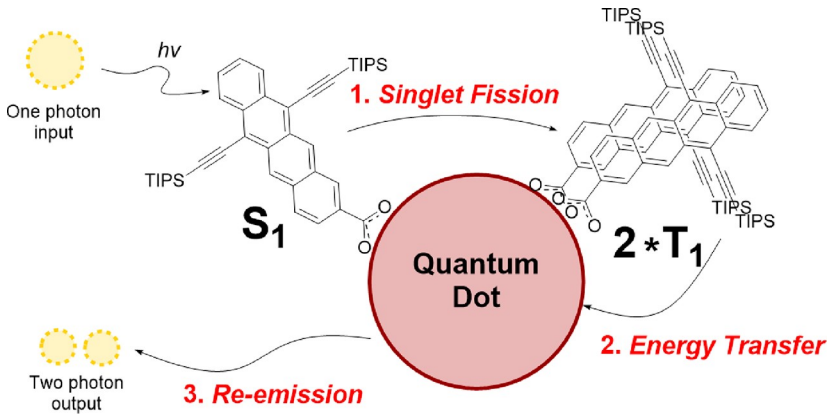

Figure 16. SF based photon-multiplier utilizing bound TIPS-tetracene and PbS QDs as demonstrated in the literature.[10,20,130]

Dworak et al.[154] formed a photochromatic hybrid system to elucidate the quenching mechanisms taking place in the donor. Assembly of the hybrid system can cause a loss of passivation of the QD donor, thus giving rise to a quenching effect that could be mistaken for energy transfer. The authors begun by choosing CdSe QDs as a donor for its well-established FRET and ligand exchange ability.[13,146−155,157,159,160,163,164,186] The authors then chose a photochromatic dye, dithienylethene dye (DTE), as their acceptor candidate to be bound (Figure 15). An adamantyl based tripodal linker furnished with three COOH anchoring groups was utilized for binding between donor and acceptor. Ligand exchange was performed in chloroform over 15 min using specific amounts of each component, the resultant hybrid system was isolated by syringe filtration. In the open form (o-DTE), DTE cannot perform FRET, conversely the closed or photo stationary form (pss-DTE) can perform FRET. The open and closed form was accessed by 590 and 320 nm illumination, respectively. The authors examined the emissive lifetime of the donor for: CdSe, CdSe/o-DTE, and CdSe/pss-DTE. In both the CdSe/o-DTE and CdSe/pss-DTE systems, quenching was observed relative to CdSe. In CdSe/o-DTE, this quenching is attributed to decreased passivation of the donor, whereas in CdSe/pss-DTE the quenching is attributed to FRET and decreased passivation of the donor. This enabled the authors to directly estimate a FRET efficiency by comparing how the CdSe/pss-DTE system quenches relative to the CdSe/o-DTE system, resulting in an efficiency of ≈81%. Being able to discriminate between the quenching mechanisms taking place in a hybrid system made these findings the first of their kind, and naturally they have important implications for FRET based hybrid systems when quantifying FRET efficiencies.

8.2. Singlet Fission

Singlet fission (SF) is a process that can occur in some organic chromophores, converting one singlet excited state of the chromophore into two triplet excited states.[187] This process offers promise to increase the number of excited states reaching a photovoltaic from solar excitation.[10,135] Two types of HN system have been employed with SF chromophores. The first involves triplet energy transfer from the chromophore to QD, aiming to emit the SF generated excited states, acting as a photon multiplier (Figure 16).[10,20,21,130,188] The second involves energy transfer from QD to chromophore, sensitizing SF for wavelengths where the chromophore has poor absorption.[18]

Recent progress of the photon multiplication process has focused on transferring the dark triplet states from SF chromophores into QDs where quantum confinement effects introduce a triplet like ground state in the QD,[189] allowing emission.[135] The initial work on QD doped tetracene (a chromophore that exhibits excellent SF efficiencies) films exhibited significant loss mechanisms due to inefficient triplet transfer through insulating ligands.[135] This led to interest in a HN system, with a SF chromophore directly attached to an emissive QD to act as a photon multiplier system.[10,21,130,188]

Davis et al.[10] demonstrated the first example of a HN system using a SF chromophore, directly attaching a TIPS-tetracene carboxylic acid ligand, 6,11-bis((triisopropylsilyl)ethynyl)-tetracene-2-carboxylic acid, to the surface of PbS QDs (Figure 16).[10] While SF in the molecule chosen had yet to be measured, SF in tetracene is known to be up to 200% efficient.[187] To allow triplet energy transfer from tetracene to the QD, the band gap energy of the QD must be lower than the triplet energy of TIPS-tetracene (∼1.25 eV).[19] In addition to this, the excitons transferred need to be re-emitted, meaning a high PLQE QD is desired. Lead sulfide nanoparticles have shown the ability to be broadly tuned across the near-infrared region,[35] with moderate PLQEs between 10−60% depending on the band gap energy.[190] As a result of these properties, PbS QDs with a band gap of 0.93 eV were selected.[10] Since triplet energy transfer proceeds via short-range Dexter energy transfer,[10] including a shell and linker would increase the distance between the chromophore and QD, reducing the transfer efficiency.[10] The binding group was selected as a carboxylic acid,[10] a well-known binding group for PbS QD ligands.[35,135] Following attachment of the TIPS-tetracene carboxylic acid to the surface of the PbS QDs, analysis showed that SF and triplet transfer was occurring with near 200% efficiency.[10] However, functionalization of the PbS reduced the PLQE of the particles, resulting in an overall photon multiplication efficiency of just 17%.[10]

Since this first publication showing the potential for a HN system to act as a photon multiplier, further investigations into this system have been carried out. A thiol functionalized TIPS-tetracene, 6,11-(bis((triisopropylsilyl)ethynyl)tetracen-2-yl)-methanethiol, was also shown to undergo efficient SF and triplet transfer to a PbS QD.[130] While the photon multiplication results were similar to the tetracene carboxylic acid, the thiol was proposed to bind more strongly to the surface of the PbS QD, accounting for the improved thermal stability.[130] This thiol also employed a small single carbon linker between

https://doi.org/10.1021/acsphyschemau.2c00018
ACS Phys. Chem Au 2022, 2, 364−387

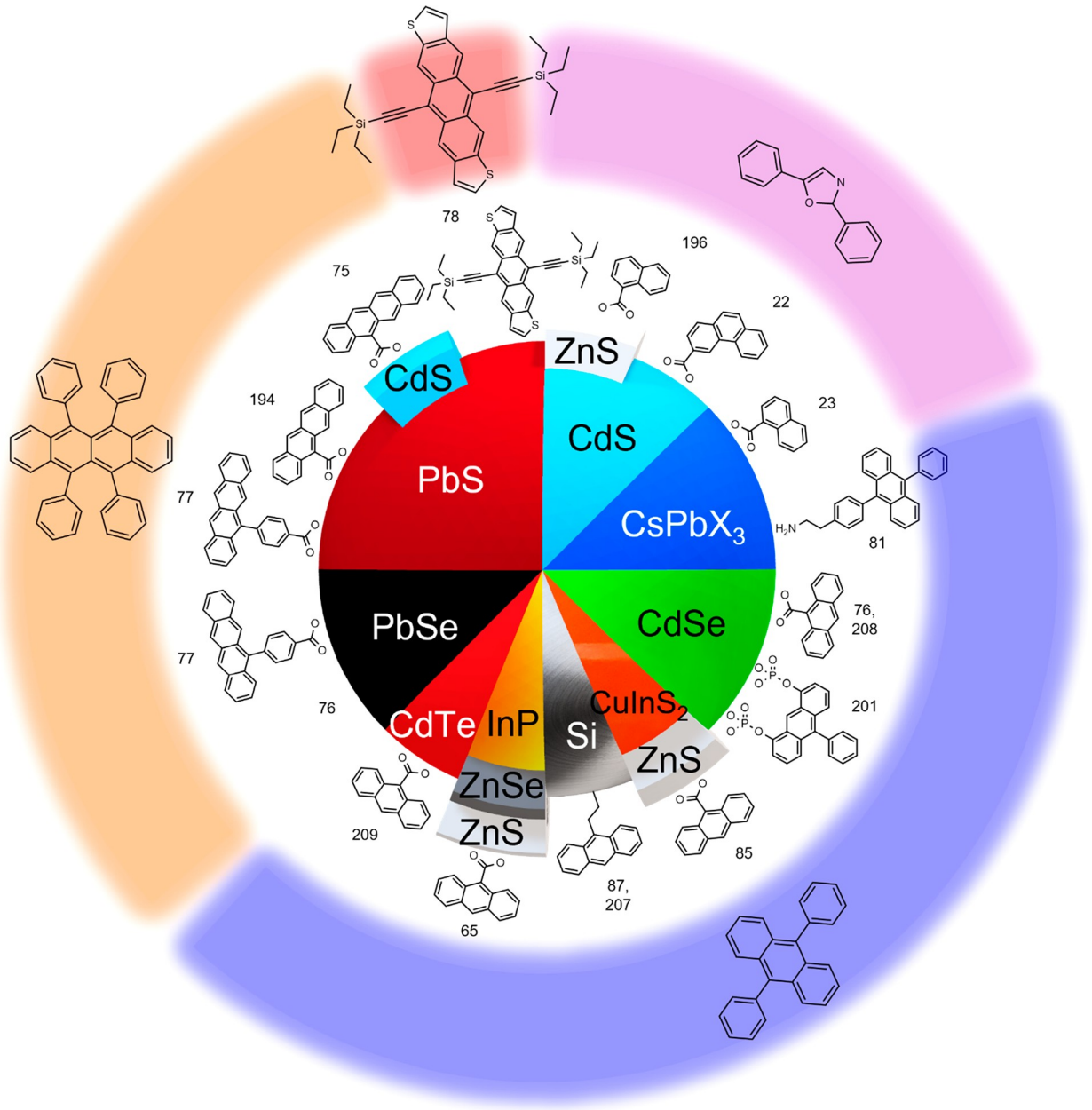

Figure 17. Visual summary of all HNs of upconversion that will be discussed in this following section. References of presented research are displayed as numbers around the image.

chromophore and binding group, although this was only necessary for the synthetic route used to the ligand.[130]

A challenge with SF chromophores is the limited absorption range they cover, reducing the portion of high energy photons that can undergo SF.[18] For example, pentacene has little to no absorption in the 400−500 nm region.[18] To improve absorption in this region, a HN system was utilized, attaching a TIPS-pentacene carboxylic acid to a $CsPbBr_3$ perovskite QD.[18] Like the TIPS-tetracene carboxylic acid system discussed above, no linker or shell was included and the chromophore was bound to the QD using a carboxylic acid. Again, short-range dexter energy transfer occurred, although in this case from QD to chromophore, where SF could then take place. They found that excitation of the perovskite QD ultimately led to the formation of triplet excited states in the SF chromophore, indicating that the hybrid system successfully sensitized SF.[18] Future work is needed to allow for extraction of the generated triplets following sensitization.

Overall, the inclusion of HNs in the SF area has drastically improved the outlook for utilization of the SF process. The ability for a process such as SF to occur at the surface of a QD is powerful and may have a range of future impacts across other fields. The biggest challenge facing SF HN systems is the reduction of QD PLQE when attaching the SF chromophore to the surface. Future work is also needed to transition to higher PLQE QDs so that photon multiplication efficiencies approaching 200% can be achieved. If this is possible, then these SF HN systems could be broadly applied to existing solar panels to increase efficiency.[21,188]

8.3. Upconversion

Upconversion in organic/inorganic HNs takes advantage of triplet−triplet annihilation (TTA), an energy transfer mecha-

https://doi.org/10.1021/acsphyschemau.2c00018
ACS Phys. Chem Au 2022, 2, 364−387

nism that occurs between two molecules in their triplet excited states, producing a singlet ground state (S_0) and an emissive singlet excited state (S_1). The exact mechanism of TTA will not be described in this text, but more information can be found in a report by Bossanyi et al.[191] As direct excitation from the singlet ground state to the first triplet excited state is a spin forbidden process, it is necessary to "sensitize" the triplet states of the annihilator with another compound that can efficiently produce triplet excited states and transfer them.[192] Inorganic semiconductors possessing a significant heavy metal content can fulfill this role as the spin−orbit interaction can convert photogenerated singlet excitons into triplets with minimal energy penalty (<15 meV).[193−197] These triplets can then undergo triplet energy transfer (TET) to nearby annihilators in solution that possess the appropriate triplet energy state.

While not present in all HN upconversion systems, it is common to have a third component which is commonly referred to as a mediator or transmitter ligand.[22,76] The mediator ligand is a chemical species that facilitates TET between the sensitizer and annihilator[191] by allowing triplets to transition through the ligand shell[76,168] and increasing the lifetime of the photoproduced triplets by up to 6 orders of magnitude.[25,198−200] In the literature, it is common to report the upconversion efficiency as a percentage out of 100%. However, in terms of a photons absorbed versus photons emitted, the maximum PLQE of a TTA based conversion system is 50%, as two photons are required to produce one upconverted photon. Therefore, most reported upconversion efficiencies are the PLQE of the upconversion system multiplied by two. It must be pointed out, that there is debate among the community about merits of this practice.[201] In this Review, the reported "upconversion efficiency" will be referenced as opposed to the traditional quantum yield.

There are several potential applications for photon upconversion including the production of UV light, deep tissue bioimaging, and increasing the efficiency of photovoltaic cells.[22,23,202] The intended application heavily dictates the three components of the HN, but this is heavily dictated by the annihilator as that controls the emission wavelength. A tabulation of commonly utilized annihilators can be viewed in Table 2 and Figure 17.

8.3.1. Upconversion of Visible to UV Light. The upconversion of visible to UV light has been achieved in several organic/inorganic HNs. In such systems, the sensitizer is usually a wide band gap QD such as cadmium sulfide (CdS), cadmium selenide (CdSe), or quantum confined cesium lead bromide ($CsPbBr_3$).[22,23,76,202] The annihilator is usually 2,5-diphenyloxazole (PPO) with a peak emission wavelength of 355 nm and a fluorescence quantum yield of between 85 and 95%.[22,203,204]

The first such example was developed by Gray et al.[202] which involved the use of CdS QDs in solution with PPO annihilator. The CdS QDs were synthesized via a hot-injection method with a passivating ZnS shell ranging from 0 to 6 monolayers. PLQEs increased from near 0 to a maximum of 26% with a shell thickness of 4 monolayers (Figure 18). The QDs were then functionalized with naphthalene-1-carboxylic acid (1-NCA) to act as the mediator ligand. With pure, unshelled, CdS QDs, a low upconversion efficiency (Φ'_{UC}) of 0.8% was observed, a likely consequence of the lack of surface defect passivation, resulting in significant nonradiative decay which competes with TET. The addition of just one monolayer of ZnS passivation resulted in a small improvement in upconversion, though the highest upconversion efficiency of 5.2 ± 0.5% was achieved with a shell thickness of 4 monolayers, which also correlates with the highest QD PLQE and therefore the lowest rate of nonradiative decay (see Figure 18). While it would be simple to conclude that further passivation should further increase the upconversion efficiency, it should be noted that shelling material such as ZnS has been shown to be a tunnelling barrier to TET.[206] Though not found in this example, a study which utilized PbS QDs with a CdS shell found that 0.1 nm is the ideal shell thickness for maximizing upconversion efficiency. Beyond this thickness, the shell hinders TET.[75]

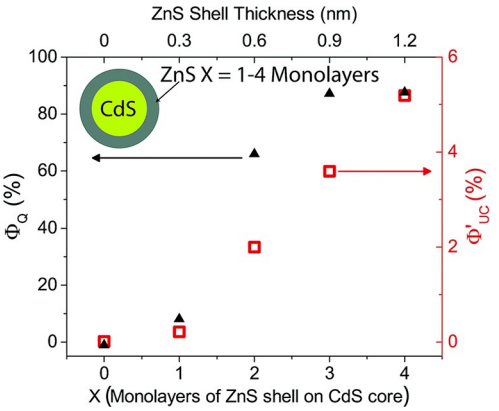

Figure 18. Plot of ZnS shell thickness, CdS/ZnS PLQE, and upconversion efficiency. Reprinted with permission under a Creative Commons Attribution 3.0 Unported License from ref 202. Copyright 2017 Royal Society of Chemistry.

It should be noted that the shelling of QDs is not required for efficient upconversion as shown by several studies.[22,207] An upconversion efficiency of 10.4% can be achieved utilizing high quality, nonshelled CdS cores[22] (which can be synthesized with a PLQE between 19.6 and 27.5%[208]) and a PPO annihilator. In this case, the mediator ligand was phenanthrene-3-carboxylic acid (3-PCA) which possesses a higher triplet energy than 1-NCA, therefore providing a stepped energetic gradient between the mediator ligand and the annihilator.[22]

An alternative to CdS/ZnS QDs as a sensitizer for upconversion is lead halide perovskite NCs. Due to their defect tolerance, perovskite NCs do not require a shell to achieve high PLQEs. He et al.[23] demonstrated that quantum-confined $CsPbBr_3$ perovskite NCs, functionalized with 1-NCA, can efficiently sensitized PPO, resulting in an upconversion efficiency of 10.2%. When utilizing perovskites as a sensitizer for TTA, it is important to synthesis NCs of a sufficiently small size, as the efficiency of TET and subsequently upconversion increases as the size of the sensitizer decreases.[209−211] While this is true for all QDs, it is particularly crucial for perovskite NCs as most methods of synthesis produce NCs that are larger in size than the bohr radius (5 nm for $CsPbCl_3$, 7 nm for $CsPbBr_3$, and 12 nm for $CsPbI_3$).[79,212]

The importance of quantum confinement, and thus NC size, for TET when utilizing perovskite NCs is highlighted by the upconversion system developed by Mase et al.[81] In this system, $CsPbI_xBr_{3-x}$ NCs in conjunction with the annihilator 9,10-diphenylanthracene (DPA) enable the upconversion of 532 nm excitation into 443 nm emission. TET was facilitated by performing a ligand exchange to functionalize the surface of the NCs with 2-(4-(10-phenylanthracen-9-yl)phenyl)ethan-1-

https://doi.org/10.1021/acsphyschemau.2c00018
ACS Phys. Chem Au 2022, 2, 364−387

amine, an ethylamine functionalized derivative of DPA (here referred to as DPA*). However, the upconversion efficiency of the system was only 1.5%, which is much lower than that of both the previously discussed $CsPbBr_3$/1-NCA/PPO system and a comparable CdSe/ACA/DPA system developed by Huang et al.[76] which achieved an upconversion efficiency of 9 ± 2%.

In the system developed by Huang et al.,[76] the annihilator is the same as that utilized in the system developed by Mase et al.;[81] however, both the utilized sensitizer and mediator ligands differ. Comparing the energetic separation between the sensitizer and mediator ligands, the perovskite/DPA* pair has a smaller separation of 0.22 eV versus the 0.46 eV of the CdSe/ACA pair (Figure 19). Considering the closer energetic

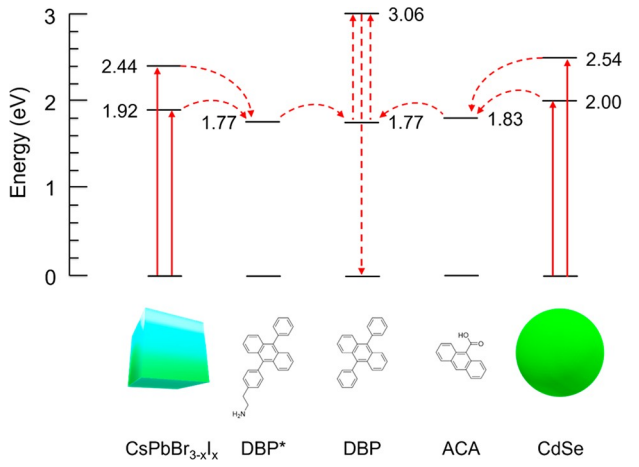

Figure 19. Energy level diagram of the components that make up the $CsPbI_xBr_{3-x}$/DPA*/DPA (left) and the CdSe/ACA/DPA (right) upconversion HNs.[81,211]

alignment between the perovskite and DPA* versus CdSe and ACA, and the higher PLQE of perovskite at over 65% versus the 12% for CdSe, it would be expected that the upconversion efficiency of the perovskite based system would be better than that of the CdSe system.

There are two possible reasons for the dramatic difference in UC efficiency between the $CsPbI_xBr_{3-x}$/DPA*/DPA system and the CdSe/ACA/DPA system. (1) As DPA is both the mediator and annihilator, there is no significant energetic gradient for TET, whereas ACA/DPA has a 60 meV difference. (2) The perovskite NCs were 7.5 ± 1.7 nm and therefore not sufficiently quantum confined to allow for effective TET. Given that 60 meV offers only a small driving force, it is likely that the lack of quantum confinement is the main cause for the efficiency difference. This comparison highlights how an upconversion system can be optimized to improve upconversion efficiency.

As shown by De Roo et al.,[207] the upconversion efficiency of a CdSe/DPA system can be improved further by replacing ACA with 10-phenyl-anthracene-1,8-diyl (dihydrogen phosphate) (Ph-ADP). The authors observe both a faster rate of TET between CdSe and Ph-ADP than for CdSe and ACA and an improved upconversion efficiency of 16.9%. The faster rate of TET is attributed to the lower lying triplet energy of the mediator ligand, while the higher upconversion efficiency is a consequence of the increased triplet lifetime of Ph-ADP at 299.9 ± 9.5 μs versus the 88.2 ± 2.1 μs for ACA. The longer triplet lifetime is theorized to be the result of lower rates of nonradiative recombination, as indicated by the higher PLQE of 76% of Ph-ADP versus the 43.2% for ACA.[207] Low rates of nonradiative recombination and therefore increased triplet lifetimes is beneficial to the final TET to the annihilator.

Besides cadmium chalcogenides and lead halide perovskites, tertiary copper indium sulfide NCs (CIS NCs) have also been incorporated as sensitizers in HN upconversion systems, with impressive results.[85] The CIS NCs were synthesized via a thiol free method, as the presence of thiol based ligands prevented ligand exchange due to the high affinity of thiols for the NCs surface. The CIS NCs were coated with a thin ZnS shell to passivate the surface, an ACA mediator ligand was then coupled to the core/shell NCs, and the final sensitizer/mediator hybrid was mixed into a solution with the annihilator DPA. This system produced an upconversion efficiency of 18.6 ± 0.3%, which, at the time of writing, is the highest upconversion efficiency for a hybrid organic/inorganic nanomaterial. The high efficiency is attributed to the good mediator/annihilator pair and to the unusually long lifetime of self-trapped excitons within CIS NCs (209 ± 17 ns) which resulted in a TET efficiency from the CIS/ZnS sensitizer to the mediator ligand of 92.3%.[85]

A drawback to the use of CIS NCs is that the emission is the result of self-trapped excitons which results in a significant energy loss between the initial excitation and the final emission. Alternative nontoxic triplet sensitizers involve the use of silicon (Si) QDs and shelled indium phosphide (InP). Silicon NCs can be thermally hydrosilylated in the presence of 9-vinylanthracene which functionalizes the surface of the NC with triplet accepting anthracene. While in the presence of DPA, the system is able to upconvert 532 and 640 nm light into violet DPA emission with an upconversion efficiency of 7 ± 0.9%[87] which was further increased to 15% in a subsequent study in the following year by preventing oxygen induce quenching.[213] However, due to the indirect band gap of silicon, the sensitizer is ineffective at absorbing wavelengths above 400 nm, making for a poor sensitizer at low excitation densities.

InP QDs have also been shown to sensitize TTA in DPA when coupled to ACA ligands.[65] To reduce nonradiative decay, the InP QDs were shelled with ZnSe and ZnS. The upconversion efficiency of this InP-ZnSe-ZnS/ACA/DPA system was 10 ± 0.1% when excited with 530 nm light, which exceeds the efficiency of the equivalent system developed by Huang et al.[76] which utilized unshelled CdSe.

All examples discussed so far have utilized zero-dimensional QDs,; however, several studies have been performed on higher dimensional nanomaterials, such as two-dimensional nanoplatelets and one-dimensional nanorods. CdSe nanoplatelets can be coupled to 9ACA mediator ligands and sensitizer DPA, just as standard CdSe QDs can, with an upconversion efficiency of 5.4%.[214] Vanorman et al.[215] demonstrated successful upconversion utilizing cadmium telluride nanorods which were functionalized with 9ACA mediator ligands, with the DPA annihilator. CdTe was chosen as the sensitizer to allow for a narrower band gap while still maintaining sufficient quantum confinement to enable efficient TET.[215] This system was shown to be capable of converting 520 nm excitation into blue DPA emission with an upconversion efficiency of 4.3%.

8.3.2. Upconversion of Near Infrared to Visible Light.

The upconversion of infrared light to visible photons is an area of intense research due to its potential to increase the efficiency of photovoltaics cells above the Shockley−Queisser Limit.[216] As the band gap of a typical silicon photovoltaic is 1.1−1.3 eV,

https://doi.org/10.1021/acsphyschemau.2c00018
ACS Phys. Chem Au 2022, 2, 364−387

any photon with an energy less than this will not be absorbed.[217] Upconversion offers the possibility of converting this energy into harvestable shorter wavelength photons. For this application, HNs are well suited as PbS and PbSe QDs have tunable absorption ranges that extend well into the near-infrared spectral region. Additionally, molecules such as rubrene are capable of TTA and have triplet energies of 1.1 eV, allowing them to accept triplet states from lead chalcogenide QDs of an appropriate size.

The first example of near-infrared upconversion utilizing an organic/inorganic HN was developed by Huang et al.[76] and was composed of PbSe QDs as the sensitizer and rubrene as the annihilator (Figure 20). With both components in

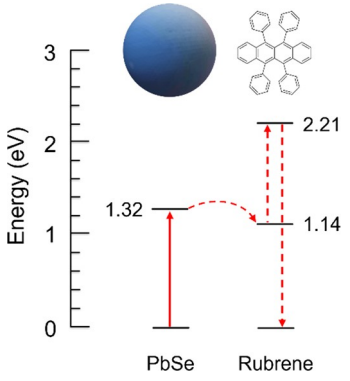

Figure 20. Energy level diagram of the PbSe/Rubrene upconversion HN.[76]

degassed toluene, excitation of the QDs with both 808 and 980 nm laser light resulted in the bright yellow emission of rubrene. However, the upconversion efficiency was only 0.01% which the authors argue was due to the lack of a mediator ligand. This conclusion was proven correct when the same group introduced a mediator ligand in the form of 4-(tetracen-5-yl)benzoic acid (abbreviated to CPT) which has a triplet energy of 1.16 eV, above that of the annihilator at 1.14 eV. The addition of CPT to the PbSe/rubrene system increased the upconversion efficiency 11-fold, from 0.20 to 2.1%. Note that this is with an excitation wavelength of 808 nm. The researchers simultaneously also experimented with PbS QDs, demonstrating an even more dramatic increase in upconversion efficiency with the addition of a mediator ligand, from 0.021 to 1.7%.[77]

As with cadmium chalcogenide QDs, nonradiative decay in lead chalcogenide QDs can be reduced via the growth of a passivating shell, typically CdS.[218] Via the use of a CdS shell along with a 5-carboxylic acid tetracene (5-CAT) ligand as a mediator ligand, Mahboub et al.[75] was able to increase the upconversion efficiency of a PbS/rubrene system to 8.4 ± 1%.[75] The same system was tested without the mediator ligand, and as expected the upconversion efficiency dropped significantly to a maximum of ∼0.085%, which correlated with a CdS shell thickness of 0.1 nm (Figure 21). A further increase in shell thickness results in lower upconversion efficiency, demonstrating that there is a point where the potential increase in QD PLQE is offset by the tunnelling barrier presented by the shell.

However, as with CdS QDs, a passivating shell is not necessary to achieve efficient upconversion when utilizing PbS QDs. By synthesizing high quality PbS QDs via the use of high purity reagents, Huang et al.[200] was able to achieve an upconversion efficiency of 11.8 ± 1.1% with a PbS/5-CAT/Rubrene system.[200] Additionally, the authors also found that the surface chemistry of the QD is significant factor in terms of the final upconversion efficiency. PbS QDs were made via two methods, one which uses a thiourea as the sulfur precursor and another which uses hexamethyldisilathane. In the original publication, the two sets of QDs are referred to as PbS-T for the dots synthesized with thiourea and PbS-S for those synthesized with hexamethyldisilathane. An upconversion system that uses PbS-T QDs achieves an almost 12% upconversion efficiency, while the use of the PbS-S QDs only achieves an upconversion efficiency of 4.6 ± 0.4% (Figure 22). The difference in upconversion efficiency is not due to the difference in quality of the dots, as both possess comparable PLQEs of 34.1 ± 1.3 and 29.5 ± 1.2%, respectively. The difference arises in the lifetime of the triplet excited state of the 5-CAT ligands. When 5-CAT is bound to PbS-T, the lifetime of the triplet excited state is measured to be 2.86 μs, while it is 10 times shorter at 0.27 μs when 5-CAT is bound to PbS-S. The authors argue that there is a difference in the surface chemistry between PbS-T and PbS-S QDs that influences the heavy atom effect on the triplet lifetime of the ligands, though they could not speculate exactly what the difference in surface chemistry was.

One drawback of the use of a mediator ligand is that a larger energy difference between the sensitizer and annihilator is required to provide enough of an energetic gradient to facilitate each TET step. In theory, by eliminating the use of a

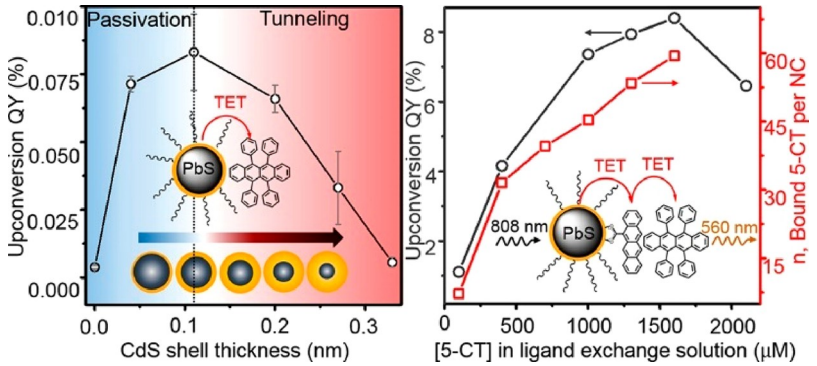

Figure 21. Plots showing the relationship between QD shell thickness and upconversion efficiency. Reprinted from ref 75. Copyright 2016 American Chemical Society.

https://doi.org/10.1021/acsphyschemau.2c00018
ACS Phys. Chem Au 2022, 2, 364−387

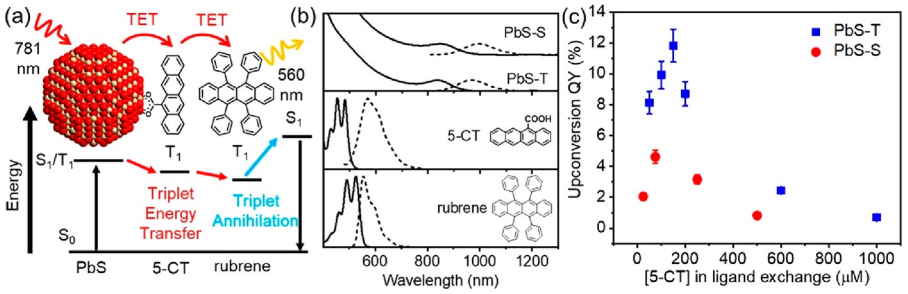

Figure 22. (a) Energy level diagram of the PbS/5-CT/Rubrene upconversion HN. (b) Absorbance and PL of two samples of PbS QDs, 5-CT mediator ligand, and rubrene annihilator. (c) Plot of upconversion efficiency versus the concentration of mediator ligand for two PbS/5-CT/Rubrene systems.[200] Reprinted from ref 200. Copyright 2019 American Chemical Society.

mediator ligand, QDs with narrower band gaps could be utilized, allowing for longer wavelengths to be harnessed. To address this issue, Nishimura et al.[78] sought to use an annihilator that could reversibly bind and unbind to the QD. Due to the lack of binding functionality, rubrene could not be used for this purpose and the authors instead utilized bis(triethylsilylethylnyl)-anthradithiophene (TES-ADT), a heterocyclic aromatic compound which possesses sulfur atoms that can bind to the surface of lead chalcogenide QDs. Due to the lack of a mediator ligand, large PbS QDs were able to be utilized, allowing for excitation with wavelengths up to 1064 nm. While the efficiency of TET to TES-ADT is higher at 12 ± 2% versus the 0.02% to rubrene, and the authors suggest that detachment of the ligand was occurring, a maximum upconversion efficiency of only 0.012% was achieved.[78]

8.3.3. Overall HN design for UC. Efficient upconversion using hybrid organic/inorganic nanomaterials requires several factors from each component of the system. First, with regard to the sensitizer, the most important factor is sufficient quantum confinement which is found to be crucial for effective TET.[209−211] Additional benefits include high PLQEs and long triplet lifetimes.[22,23,87] For mediator ligands, it is important that there is a close energetic alignment between the triplet energy states of the ligand and the other components of the system to allow for both effective TET and to minimize the loss in energy between the initial triplet excited state in the sensitizer and the final triplet state in the annihilator.[22] Simultaneously, it is beneficial to the efficiency of TET to have a steep energetic gradient between the mediator ligand and annihilator to facilitate the final TET step.[22,76] For the annihilator, efficient TTA requires a high PLQE to maximize the final emission event.[22] As there is a limited number of effective annihilators, it is much easier to adjust the sensitizer and mediator ligands of the system to maximize the upconversion efficiency. A tabulation of the discussed hybrid organic/inorganic nanomaterials can be viewed in Table 3, and a visual representation of this table can be viewed in Figure 17 at the beginning of this section.

8.4. Thermally Activated Delayed Fluorescence

Thermally activated delayed fluorescence (TDAF) is the process in which a system can incorporate thermal energy to transition from a nonemissive state into an emissive state.[219−221] In hybrid organic/inorganic systems, TDAF can be achieved via the population of triplet states in surface bound organic chromophores via an energetically favorable TET from a QD and then a subsequent thermally activated reverse TET (rTET) back to the original donor from which delayed emission can occur.[70,82] In essence, an equilibrium between forward and reverse TET can develop between the components of the HN.

Table 3. Summary Table of the Discussed Upconversion Systems

sensitizer	mediator	annihilator	excitation (nm)	upconversion efficiency (%)
CdS/ZnS[202]	1-NCA	PPO	405	5.2 ± 0.2
CdS[22]	3-PCA	PPO	405	10.4
$CsPbBr_3$[23]	1-NCA	PPO	443	10.2
$CsPbBr_xI_{3-x}$[81]	DPA*	DPA	532	1.5
CdSe[76]	ACA	DPA	532	9 ± 2
CdSe[207]	Ph-ADP	DPA	488	16.9
$CuInS_2$/ZnS[85]	ACA	DPA	520	18.6 ± 0.9
Si[87,213]	anthracene	DPA	488	15
InP/ZnSe/ZnS[65]	ACA	DPA	530−590	10 ± 0.1
CdSe (platelets)[214]	ACA	DPA	532	5.4
CdTe (nanorods)[215]	ACA	DPA	520	4.3
PbSe[76]		rubrene	808−980	0.01
PbSe[77]	CPT	rubrene	808	2.1
PbS[77]	CPT	rubrene	808	1.7
PbS/CdS[75]	5-CAT	rubrene	808	8.4 ± 1
PbS[200]	5-CAT	rubrene	781	11.8 ± 1.1
PbS[78]		TES-ADT	647−1064	0.012

To enable efficient thermally activated rTET, the energy separation between the triplet state of the chromophore and the conduction band minimum of the QD must be within a certain energy threshold. This fact was shown by Mongin et al.[70] who synthesized unshelled CdSe QDs of various band gap values (as indicated by the PL signal) which they functionalized with pyrene carboxylic acid (PCA) ligands. For the QD sample with the widest band gap (488 nm PL), the energy separation between the conduction band minimum of the QD and triplet excited state of the ligand was 0.54 eV and no back transfer would occur as indicated by the fully quenched CdSe emission which was determined to have a photoluminescence quantum efficiency of ≤1%. Only after decreasing the band gap would rTET activate. A maximum TADF was observed for QDs that exhibited 600 nm PL which corresponded to an energy separation of 0.07 eV (70 meV). In this scenario, the PLQE of TDAF in the CdSe QDs was 13%.[70] Additionally, the lifetime of QD emission increased dramatically. For unshelled CdSe, the typical fluorescence lifetime is on the order of 10^1 ns.[222] However, with the coupling of PCA, this lifetime can be increased to between 1.57 ± 0.02 μs and 52 ± 2 ms.[70] Similar

https://doi.org/10.1021/acsphyschemau.2c00018
ACS Phys. Chem Au 2022, 2, 364−387

results were obtained by a later study that also coupled CdSe to PCA ligands.[223]

A second example of TDAF in a hybrid organic/inorganic nanomaterial involves the use of quantum confined $CsPbBr_3$ NCs and phenanthrene carboxylic acid (PTA) ligands (Figure 23).[82] TET efficiencies varied with the concentration of ligand

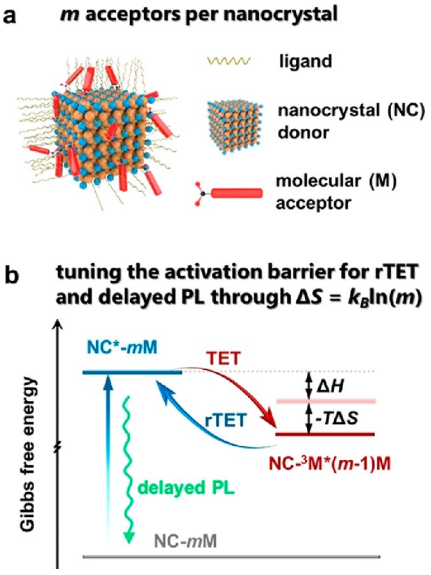

Figure 23. Energy levels and TADF mechanism of the HN $CsPbBr_3$–PTA.[82] Reprinted from ref 82. Copyright 2021 American Chemical Society.

in solution with values between 13.1 and 63.2% were reported, though no reverse TET efficiencies were reported. The lifetime of perovskite emission is typically on the order of 1–29 ns.[79] However, when coupled to PTA ligands, the lifetime can be increased to ~35 μs at the highest ligand concentration.[82]

At the time of writing, these are the only three examples of TDAF in hybrid organic/inorganic nanomaterials. Due to this, there is plenty of opportunity for further refinement of these systems. As Mongin et al.[70] mention in their concluding remarks, the use of unshelled CdSe allows for competitive nonradiative recombination mechanisms and therefore the use of a passivating shell would be a next step forward for future investigations. Additionally, TDAF in HNs has only been demonstrated in a narrow range of emission wavelengths (510–605 nm).

9. FUTURE

The future directions and applications of HNs will be fundamentally controlled by the material systems developed. Thus, potential must be found in the two major components of the HN, the QD and the organic semiconductor. The ability to synthesize heterodot architectures gives rise to a vast number of NC permutations, the importance of which being the ability to control passivation, Stokes shift, stability, donor–acceptor distance, excited state lifetimes, and surface chemistry. The continued growth of the field of HNs will inevitably result in the development of sophisticated heterodot architectures designed to improve HN systems. The three-component design of organic semiconductors for HN applications means that synthetic chemistry plays a vital role in optimizing chromophores. The ability to tune the binding group, linker, and chromophore independently allows for the binding strength, packing orientation, QD-chromophore distance, and chromophore to each be optimized, providing an optimal HN system. As the field of HNs continues to grow, we expect to see an increase in novel synthetic chromophores optimized for their unique applications, thus improving the properties of the HN systems.

Out of all the discussed applications, HNs for FRET are the most thoroughly studied and the closest to seeing real world applications,[6,84,142−164] with FRET efficiencies surpassing 90%. As such, current research is focused on the deployment of these HNs in practical applications, for example, sensing and solar technologies.

Efficient singlet fission in HNs is currently limited by the low PLQEs of the PbS QDs used for re-emission of the generated triplets.[10] Transitioning to higher PLQE QDs is a priority to allow for photon multiplication efficiencies to approach 200%. If possible, SF photon multiplication could be broadly used with existing solar panels to increase efficiency.

For upconversion, the limiting factor to the overall efficiency is the sequential TET from the sensitizer to the mediator ligand and from the ligand to the annihilator in solution.[224] The highest TETs have been achieved via a combination of high PLQEs and long triplet lifetimes of both the QDs sensitizer and mediator ligands.[85,207] Additionally, a steep energetic cascade also benefits TETs; however, this increases the energetic penalty of each TET step.[211] Therefore, future work will need to find the optimal triads of sensitizer, mediator, and annihilator that allows for the most efficient TET with the smallest loss in triplet excitation energy.

The application of thermally activated delayed fluorescence in HNs is relatively unexplored and has so far only been demonstrated in a very limited number of systems. As there is a wide range of possible QD/chromophore combinations, there is plenty of scope for further research in this field.

Although so far unproven, HNs may have the potential to create a new class of LED materials. It is well-known that organic light emitting diodes (OLEDs) currently suffer from electron-spin limitations and are capped at 25% efficiency.[225] This limit stems from the spin-statistics of recombination which, in general, form one emissive singlet state per three nonemissive triplet states. While QD LEDs (QDLEDs) can bypass electron-spin efficiency limits (due to 'quantum confinement effects making triplets emissive),[226,227] unfortunately the surfaces of QDs, which are usually coated by insulation molecules (ligands), hinders charge injection.[228] As such, while QDLEDs are unaffected by electron-spin limits, device efficiencies are still below those of OLEDs due to the issue of charge injection through the surface ligand shell.[229] By replacing the insulating surface ligands on a QD with OLED molecules, these new HN LEDs may exhibit increased charge injection efficiency (compared to QDLEDs) and the ability to emit from historically nonemissive triplet states (compared to OLEDs).

HNs have a promising future ahead in many research fields and technology applications. The adjustable nature of HNs has seen their successful application in various optoelectronic applications including Förster resonance energy transfer, singlet fission, upconversion, and thermally activated delayed fluorescence (as referenced above in specific sections). While the initial demonstration of each of these processes typically exhibited low efficiencies, incremental improvements of HN systems has seen these efficiencies rise, though there is still a

https://doi.org/10.1021/acsphyschemau.2c00018
ACS Phys. Chem Au 2022, 2, 364–387

need for further improvement before many of these systems see application beyond the laboratory.

AUTHOR INFORMATION

Corresponding Author

Nathaniel J. L. K. Davis − *School of Chemical and Physical Sciences, The MacDiarmid Institute for Advanced Materials and Nanotechnology, The Dodd-Walls Centre for Photonic and Quantum Technologies, Victoria University of Wellington, Wellington 6012, New Zealand;* orcid.org/0000-0003-2535-8968; Email: nathaniel.davis@vuw.ac.nz

Authors

Matthew W. Brett − *School of Chemical and Physical Sciences, The MacDiarmid Institute for Advanced Materials and Nanotechnology, The Dodd-Walls Centre for Photonic and Quantum Technologies, Victoria University of Wellington, Wellington 6012, New Zealand*

Calum K. Gordon − *School of Chemical and Physical Sciences, The MacDiarmid Institute for Advanced Materials and Nanotechnology, The Dodd-Walls Centre for Photonic and Quantum Technologies, Victoria University of Wellington, Wellington 6012, New Zealand;* orcid.org/0000-0002-4963-1896

Jake Hardy − *School of Chemical and Physical Sciences, The MacDiarmid Institute for Advanced Materials and Nanotechnology, The Dodd-Walls Centre for Photonic and Quantum Technologies, Victoria University of Wellington, Wellington 6012, New Zealand*

Complete contact information is available at: https://pubs.acs.org/10.1021/acsphyschemau.2c00018

Author Contributions

†These authors contributed equally to this work. All first authors (M.W.B., C.K.G., and J.H.) contributed equally to this work and their position in the author list is derived alphabetically. N.J.L.K.D. supervised and planned this manuscript.

Notes

The authors declare no competing financial interest.

ACKNOWLEDGMENTS

M.W.B. would like to thank The Victoria University Trust for a Victoria Doctorial Scholarship. C.K.G. would like to thank the Ministry of Business, Innovation and Employment for a Doctorial Scholarship. J.H. would like to thank the Science for Technological Innovation Science Challenges for a Doctorial Scholarship. N.J.L.K.D. would like to thank the Royal Society of New Zealand for a Rutherford Discovery fellowship and acknowledges research funding from the Victoria Research Trust, the Science for Technological Innovation Science Challenges, the Marsden Fund and the Ministry of Business, Innovation and Employment. We also thank Damon de Clercq for creating the blender image used for the TOC.

REFERENCES

(1) Efros, A.; Rosen, M. The Electronic Structure of Semiconductor Nanocrystals. *Annu. Rev. Mater. Sci.* **2000**, *30*, 475−521.

(2) Jin, T.; Sasaki, A.; Kinjo, M.; Miyazaki, J. A Quantum Dot-Based Ratiometric PH Sensor. *Chem. Commun.* **2010**, *46* (14), 2408−2410.

(3) Shamirian, A.; Ghai, A.; Snee, P. T. QD-Based FRET Probes at a Glance. *Sensors* **2015**, *15* (6), 13028−13051.

(4) Clegg, R. M. Förster Resonance Energy Transfer—FRET What Is It, Why Do It, and How It's Done. *Laboratory techniques in biochemistry and molecular biology* **2009**, *33*, 1−57.

(5) Sahoo, H. Förster Resonance Energy Transfer - A Spectroscopic Nanoruler: Principle and Applications. *Journal of Photochemistry and Photobiology C: Photochemistry Reviews* **2011**, *12* (1), 20−30.

(6) Thomas, A.; Nair, P. v; George Thomas, K. InP Quantum Dots: An Environmentally Friendly Material with Resonance Energy Transfer Requisites. *J. Phys. Chem. C* **2014**, *118* (7), 3838−3845.

(7) Xia, C.; Wang, W.; Du, L.; Rabouw, F. T.; J. van den Heuvel, D.; Gerritsen, H. C.; Mattoussi, H.; de Mello Donega, C. Förster Resonance Energy Transfer between Colloidal CuInS2/ZnS Quantum Dots and Dark Quenchers. *J. Phys. Chem. C* **2020**, *124* (2), 1717−1731.

(8) Hardy, J.; Brett, M. W.; Rossi, A.; Wagner, I.; Chen, K.; Timmer, M. S. M.; Stocker, B. L.; Price, M. B.; Davis, N. J. L. K. Energy Transfer between Anthracene-9-Carboxylic Acid Ligands and CsPbBr3 and CsPbI3 Nanocrystals. *J. Phys. Chem. C* **2021**, *125* (2), 1447−1453.

(9) Rossi, A.; Price, M. B.; Hardy, J.; Gorman, J.; Schmidt, T. W.; Davis, N. J. L. K. Energy Transfer between Perylene Diimide Based Ligands and Cesium Lead Bromide Perovskite Nanocrystals. *J. Phys. Chem. C* **2020**, *124* (5), 3306−3313.

(10) Davis, N. J. L. K.; Allardice, J. R.; Xiao, J.; Petty, A. J.; Greenham, N. C.; Anthony, J. E.; Rao, A. Singlet Fission and Triplet Transfer to PbS Quantum Dots in TIPS-Tetracene Carboxylic Acid Ligands. *J. Phys. Chem. Lett.* **2018**, *9* (6), 1454−1460.

(11) Vargas-Bernal, R.; He, P.; Zhang, S. *Hybrid Nanomaterials: Flexible Electronics Materials*; IntechOpen, 2020.

(12) Mazzaro, R.; Gradone, A.; Angeloni, S.; Morselli, G.; Cozzi, P. G.; Romano, F.; Vomiero, A.; Ceroni, P. Hybrid Silicon Nanocrystals for Color-Neutral and Transparent Luminescent Solar Concentrators. *ACS Photonics* **2019**, *6* (9), 2303−2311.

(13) Tummeltshammer, C.; Portnoi, M.; Mitchell, S. A.; Lee, A.-T.; Kenyon, A. J.; Tabor, A. B.; Papakonstantinou, I. On the Ability of Förster Resonance Energy Transfer to Enhance Luminescent Solar Concentrator Efficiency. *Nano Energy* **2017**, *32*, 263−270.

(14) Hammer, N. I.; Emrick, T.; Barnes, M. D. Quantum Dots Coordinated with Conjugated Organic Ligands: New Nanomaterials with Novel Photophysics. *Nanoscale Res. Lett.* **2007**, *2* (6), 282−290.

(15) Ahmad, R.; Soni, U.; Srivastava, R.; Singh, V. N.; Chand, S.; Sapra, S. Investigation of the Photophysical and Electrical Characteristics of CuInS2 QDs/SWCNT Hybrid Nanostructure. *J. Phys. Chem. C* **2014**, *118* (21), 11409−11416.

(16) Tseng, Y.-H.; He, Y.; Que, L. Ultrasensitive Thin Film Infrared Sensors Enabled by Hybrid Nanomaterials. *Analyst* **2013**, *138* (10), 3053−3057.

(17) Rathnayake, H.; White, J.; Dawood, S. Polysilsesquioxane-Based Organic-Inorganic Hybrid Nanomaterials and Their Applications towards Organic Photovoltaics. *Synth. Met.* **2021**, *273*, 116705.

(18) Lu, H.; Chen, X.; Anthony, J. E.; Johnson, J. C.; Beard, M. C. Sensitizing Singlet Fission with Perovskite Nanocrystals. *J. Am. Chem. Soc.* **2019**, *141* (12), 4919−4927.

(19) Budden, P. J.; Weiss, L. R.; Muller, M.; Panjwani, N. A.; Dowland, S.; Allardice, J. R.; Ganschow, M.; Freudenberg, J.; Behrends, J.; Bunz, U. H. F.; Friend, R. H. Singlet Exciton Fission in a Modified Acene with Improved Stability and High Photoluminescence Yield. *Nat. Commun.* **2021**, *12* (1), 1527.

(20) Allardice, J. R.; Thampi, A.; Dowland, S.; Xiao, J.; Gray, V.; Zhang, Z.; Budden, P.; Petty, A. J.; Davis, N. J. L. K.; Greenham, N. C.; et al. Engineering Molecular Ligand Shells on Quantum Dots for Quantitative Harvesting of Triplet Excitons Generated by Singlet Fission. *J. Am. Chem. Soc.* **2019**, *141* (32), 12907−12915.

(21) Futscher, M. H.; Rao, A.; Ehrler, B. The Potential of Singlet Fission Photon Multipliers as an Alternative to Silicon-Based Tandem Solar Cells. *ACS Energy Lett.* **2018**, *3* (10), 2587−2592.

(22) Hou, L.; Olesund, A.; Thurakkal, S.; Zhang, X.; Albinsson, B. Efficient Visible-to-UV Photon Upconversion Systems Based on CdS

Nanocrystals Modified with Triplet Energy Mediators. *Adv. Funct. Mater.* **2021**, *31*, 2106198.
(23) He, S.; Luo, X.; Liu, X.; Li, Y.; Wu, K. Visible-to-Ultraviolet Upconversion Efficiency above 10% Sensitized by Quantum-Confined Perovskite Nanocrystals. *J. Phys. Chem. Lett.* **2019**, *10* (17), 5036−5040.
(24) Tripathi, N.; Ando, M.; Akai, T.; Kamada, K. Efficient NIR-to-Visible Upconversion of Surface-Modified PbS Quantum Dots for Photovoltaic Devices. *ACS Applied Nano Materials* **2021**, *4* (9), 9680−9688.
(25) Xu, Z.; Huang, Z.; Li, C.; Huang, T.; Evangelista, F. A.; Tang, M. L.; Lian, T. Tuning the Quantum Dot (QD)/Mediator Interface for Optimal Efficiency of QD-Sensitized near-Infrared-to-Visible Photon Upconversion Systems. *ACS Appl. Mater. Interfaces* **2020**, *12* (32), 36558−36567.
(26) Huang, Z.; Tang, M. L. Designing Transmitter Ligands That Mediate Energy Transfer between Semiconductor Nanocrystals and Molecules. *J. Am. Chem. Soc.* **2017**, *139* (28), 9412−9418.
(27) Gray, V.; Allardice, J. R.; Zhang, Z.; Rao, A. Organic-Quantum Dot Hybrid Interfaces and Their Role in Photon Fission/Fusion Applications. *Chemical Physics Reviews* **2021**, *2* (3), 031305.
(28) Wu, J.; Chen, S.; Seeds, A.; Liu, H. Quantum Dot Optoelectronic Devices: Lasers, Photodetectors and Solar Cells. *J. Phys. D: Appl. Phys.* **2015**, *48* (36), 363001.
(29) Bhattacharya, P.; Mi, Z. Quantum-Dot Optoelectronic Devices. *Proceedings of the IEEE* **2007**, *95* (9), 1723−1740.
(30) Bhattacharya, P.; Ghosh, S.; Stiff-Roberts, A. D. Quantum Dot Opto-Electronic Devices. *Annu. Rev. Mater. Res.* **2004**, *34*, 1−40.
(31) Alivisatos, A. P. Semiconductor Clusters, Nanocrystals, and Quantum Dots. *Advancement Of Science* **1996**, *271* (5251), 933−937.
(32) Kudera, S.; Carbone, L.; Manna, L.; Parak, W. J. Growth Mechanism, Shape and Composition Control of Semiconductor Nanocrystals. In *Semicoductor Nanocrystal Quantum Dots*; Rogach, A. L., Ed.; Wiley: Vienna, 2008; pp 1−34. .
(33) Brown, P. R.; Kim, D.; Lunt, R. R.; Zhao, N.; Bawendi, M. G.; Grossman, J. C.; Bulovic, V. Energy Level Modification in Lead Sulfide Quantum Dot Thin Films through Ligand Exchange. *ACS Nano* **2014**, *8* (6), 5863−5872.
(34) Kumar, D. S.; Kumar, B. J.; Mahesh, H. M. Quantum Nanostructures (QDs): An Overview. In *Synthesis of Inorganic Nanomaterials*; Elsevier, 2018; pp 59−88.
(35) Hines, M. A.; Scholes, G. D. Colloidal PbS Nanocrystals with Size-tunable Near-infrared Emission: Observation of Post-synthesis Self-narrowing of the Particle Size Distribution. *Adv. Mater.* **2003**, *15* (21), 1844−1849.
(36) Murray, C. B.; Kagan, C. R.; Bawendi, M. G. Synthesis and Characterization of Monodisperse Nanocrystals and Close-Packed Nanocrystal Assemblies. *Annu. Rev. Mater. Sci.* **2000**, *30*, 545−610.
(37) de Mello Donegá, C.; Liljeroth, P.; Vanmaekelbergh, D. Physicochemical Evaluation of the Hot-injection Method, a Synthesis Route for Monodisperse Nanocrystals. *Small* **2005**, *1* (12), 1152−1162.
(38) Kwon, S. G.; Hyeon, T. Formation Mechanisms of Uniform Nanocrystals via Hot-injection and Heat-up Methods. *Small* **2011**, *7* (19), 2685−2702.
(39) Leatherdale, C. A.; Woo, W. K.; Mikulec, F. V.; Bawendi, M. G. On the Absorption Cross Section of CdSe Nanocrystal Quantum Dots. *J. Phys. Chem. B* **2002**, *106* (31), 7619−7622.
(40) Moreels, I.; Lambert, K.; De Muynck, D.; Vanhaecke, F.; Poelman, D.; Martins, J. C.; Allan, G.; Hens, Z. Composition and Size-Dependent Extinction Coefficient of Colloidal PbSe Quantum Dots. *Chem. Mater.* **2007**, *19* (25), 6101−6106.
(41) Moreels, I.; Lambert, K.; Smeets, D.; De Muynck, D.; Nollet, T.; Martins, J. C.; Vanhaecke, F.; Vantomme, A.; Delerue, C.; Allan, G.; Hens, Z. Size-Dependent Optical Properties of Colloidal PbS Quantum Dots. *ACS Nano* **2009**, *3* (10), 3023−3030.
(42) Cademartiri, L.; Montanari, E.; Calestani, G.; Migliori, A.; Guagliardi, A.; Ozin, G. A. Size-Dependent Extinction Coefficients of PbS Quantum Dots. *J. Am. Chem. Soc.* **2006**, *128* (31), 10337−10346.
(43) Bae, W. K.; Joo, J.; Padilha, L. A.; Won, J.; Lee, D. C.; Lin, Q.; Koh, W.; Luo, H.; Klimov, V. I.; Pietryga, J. M. Highly Effective Surface Passivation of PbSe Quantum Dots through Reaction with Molecular Chlorine. *J. Am. Chem. Soc.* **2012**, *134* (49), 20160−20168.
(44) Padilha, L. A.; Stewart, J. T.; Sandberg, R. L.; Bae, W. K.; Koh, W.-K.; Pietryga, J. M.; Klimov, V. I. Aspect Ratio Dependence of Auger Recombination and Carrier Multiplication in PbSe Nanorods. *Nano Lett.* **2013**, *13* (3), 1092−1099.
(45) Wanger, D. D.; Correa, R. E.; Dauler, E. A.; Bawendi, M. G. The Dominant Role of Exciton Quenching in PbS Quantum-Dot-Based Photovoltaic Devices. *Nano Lett.* **2013**, *13* (12), 5907−5912.
(46) Arya, H.; Kaul, Z.; Wadhwa, R.; Taira, K.; Hirano, T.; Kaul, S. C. Quantum Dots in Bio-Imaging: Revolution by the Small. *Biochem. Biophys. Res. Commun.* **2005**, *329* (4), 1173−1177.
(47) Hyldahl, M. G.; Bailey, S. T.; Wittmershaus, B. P. Photo-Stability and Performance of CdSe/ZnS Quantum Dots in Luminescent Solar Concentrators. *Sol. Energy* **2009**, *83* (4), 566−573.
(48) Englman, R.; Jortner, J. The Energy Gap Law for Radiationless Transitions in Large Molecules. *Mol. Phys.* **1970**, *18* (2), 145−164.
(49) Karatum, O.; Jalali, H. B.; Sadeghi, S.; Melikov, R.; Srivastava, S. B.; Nizamoglu, S.Light-Emitting Devices Based on Type-II InP/ZnO Quantum Dots (Conference Presentation). In *Light-Emitting Devices, Materials, and Applications XXIV*; International Society for Optics and Photonics, 2020; Vol. *11302*, p 113021J.
(50) Zhang, H.; Ma, X.; Lin, Q.; Zeng, Z.; Wang, H.; Li, L. S.; Shen, H.; Jia, Y.; Du, Z. High-Brightness Blue InP Quantum Dot-Based Electroluminescent Devices: The Role of Shell Thickness. *J. Phys. Chem. Lett.* **2020**, *11* (3), 960−967.
(51) Singh, R.; Akhil, S.; Dutt, V. G. V.; Mishra, N. Shell Thickness Dependent Photostability Studies of Green-Emitting "Giant" Quantum Dots. *Nanoscale Advances* **2021**, *3* (24), 6984−6991.
(52) McBride, J. R.; Pennycook, T. J.; Pennycook, S. J.; Rosenthal, S. J. The Possibility and Implications of Dynamic Nanoparticle Surfaces. *ACS Nano* **2013**, *7*, 8358−8365.
(53) Gur, I.; Fromer, N. A.; Geier, M. L.; Alivisatos, A. P. Air-Stable All-Inorganic Nanocrystal Solar Cells Processed from Solution. *Science* **2005**, *310* (5747), 462−465.
(54) Ip, A. H.; Thon, S. M.; Hoogland, S.; Voznyy, O.; Zhitomirsky, D.; Debnath, R.; Levina, L.; Rollny, L. R.; Carey, G. H.; Fischer, A.; Kemp, K. W.; Kramer, I. J.; Ning, Z.; Labelle, A. J.; Chou, K. W.; Amassian, A.; Sargent, E. H. Hybrid Passivated Colloidal Quantum Dot Solids. *Nat. Nanotechnol.* **2012**, *7* (9), 577−582.
(55) Pietryga, J. M.; Werder, D. J.; Williams, D. J.; Casson, J. L.; Schaller, R. D.; Klimov, V. I.; Hollingsworth, J. A. Utilizing the Lability of Lead Selenide to Produce Heterostructured Nanocrystals with Bright, Stable Infrared Emission. *J. Am. Chem. Soc.* **2008**, *130* (14), 4879−4885.
(56) Saeboe, A. M.; Nikiforov, A. Y.; Toufanian, R.; Kays, J. C.; Chern, M.; Casas, J. P.; Han, K.; Piryatinski, A.; Jones, D.; Dennis, A. M. Extending the Near-Infrared Emission Range of Indium Phosphide Quantum Dots for Multiplexed In Vivo Imaging. *Nano Lett.* **2021**, *21* (7), 3271−3279.
(57) Hollingsworth, J. A. Heterostructuring Nanocrystal Quantum Dots toward Intentional Suppression of Blinking and Auger Recombination. *Chem. Mater.* **2013**, *25* (8), 1318−1331.
(58) Li, Z.; Yu, L. Design of Mn-Doped CdxZn1-XSe@ ZnO Triple-Shelled Hollow Microspheres for Quantum Dots Sensitized Solar Cells with Improved Photovoltaic Performance. *Sol. Energy* **2019**, *184*, 315−322.
(59) Hanson, C. J.; Hartmann, N. F.; Singh, A.; Ma, X.; DeBenedetti, W. J. I.; Casson, J. L.; Grey, J. K.; Chabal, Y. J.; Malko, A. v; Sykora, M.; et al. Giant PbSe/CdSe/CdSe Quantum Dots: Crystal-Structure-Defined Ultrastable near-Infrared Photo-luminescence from Single Nanocrystals. *J. Am. Chem. Soc.* **2017**, *139* (32), 11081−11088.
(60) Murcia, M. J.; Shaw, D. L.; Woodruff, H.; Naumann, C. A.; Young, B. A.; Long, E. C. Facile Sonochemical Synthesis of Highly Luminescent ZnS- Shelled CdSe Quantum Dots. *Chem. Mater.* **2006**, *18* (9), 2219−2225.

https://doi.org/10.1021/acsphyschemau.2c00018
ACS Phys. Chem Au 2022, 2, 364−387

(61) Hujjatul Islam, M.; Paul, M. T. Y.; Burheim, O. S.; Pollet, B. G. Recent Developments in the Sonoelectrochemical Synthesis of Nanomaterials. *Ultrasonics Sonochemistry* **2019**, *59*, 104711.
(62) Shen, W.; Tang, H.; Yang, X.; Cao, Z.; Cheng, T.; Wang, X.; Tan, Z.; You, J.; Deng, Z. Synthesis of Highly Fluorescent InP/ZnS Small-Core/Thick-Shell Tetrahedral-Shaped Quantum Dots for Blue Light-Emitting Diodes. *J. Mater. Chem. C* **2017**, *5* (32), 8243−8249.
(63) Jo, J.; Jo, D.; Choi, S.; Lee, S.; Kim, H.; Yoon, S.; Kim, Y.; Han, J.; Yang, H. Highly Bright, Narrow Emissivity of InP Quantum Dots Synthesized by Aminophosphine: Effects of Double Shelling Scheme and Ga Treatment. *Advanced Optical Materials* **2021**, *9*, 2100427.
(64) Xie, R.; Battaglia, D.; Peng, X. Colloidal InP Nanocrystals as Efficient Emitters Covering Blue to Near-Infrared. *J. Am. Chem. Soc.* **2007**, *129* (50), 15432−15433.
(65) Lai, R.; Sang, Y.; Zhao, Y.; Wu, K. Triplet Sensitization and Photon Upconversion Using InP-Based Quantum Dots. *J. Am. Chem. Soc.* **2020**, *142* (47), 19825−19829.
(66) Ekimov, A. I.; Hache, F.; Schanne-Klein, M. C.; Ricard, D.; Flytzanis, C.; Kudryavtsev, I. A.; Yazeva, T. v; Rodina, A. v; Efros, Al. L. Absorption and Intensity-Dependent Photoluminescence Measurements on CdSe Quantum Dots: Assignment of the First Electronic Transitions. *Journal of the Optical Society of America B* **1993**, *10* (1), 100−107.
(67) Wei, H. H.-Y.; Evans, C. M.; Swartz, B. D.; Neukirch, A. J.; Young, J.; Prezhdo, O. v; Krauss, T. D. Colloidal Semiconductor Quantum Dots with Tunable Surface Composition. *Nano Lett.* **2012**, *12* (9), 4465−4471.
(68) Okumura, K.; Mase, K.; Yanai, N.; Kimizuka, N. Employing Core-Shell Quantum Dots as Triplet Sensitizers for Photon Upconversion. *Chem.—Eur. J.* **2016**, *22* (23), 7721−7726.
(69) Amemori, S.; Gupta, R. K.; Böhm, M. L.; Xiao, J.; Huynh, U.; Oyama, T.; Kaneko, K.; Rao, A.; Yanai, N.; Kimizuka, N. Hybridizing Semiconductor Nanocrystals with Metal-Organic Frameworks for Visible and near-Infrared Photon Upconversion. *Dalton Transactions* **2018**, *47* (26), 8590−8594.
(70) Mongin, C.; Moroz, P.; Zamkov, M.; Castellano, F. N. Thermally Activated Delayed Photoluminescence from Pyrenyl-Functionalized CdSe Quantum Dots. *Nat. Chem.* **2018**, *10* (2), 225−230.
(71) Zhang, X.; Zhang, Y.; Yan, L.; Wu, H.; Gao, W.; Zhao, J.; Yu, W. W. PbSe Nanocrystal Solar Cells Using Bandgap Engineering. *RSC Adv.* **2015**, *5* (80), 65569−65574.
(72) Jadhav, P. J.; Brown, P. R.; Thompson, N.; Wunsch, B.; Mohanty, A.; Yost, S. R.; Hontz, E.; Van Voorhis, T.; Bawendi, M. G.; Bulovic, V.; Baldo, M. A. Triplet Exciton Dissociation in Singlet Exciton Fission Photovoltaics. *Advanced materials* **2012**, *24* (46), 6169−6174.
(73) Gorman, J.; Pandya, R.; Allardice, J. R.; Price, M. B.; Schmidt, T. W.; Friend, R. H.; Rao, A.; Davis, N. J. L. K. Excimer Formation in Carboxylic Acid-Functionalized Perylene Diimides Attached to Silicon Dioxide Nanoparticles. *J. Phys. Chem. C* **2019**, *123* (6), 3433−3440.
(74) Bender, J. A.; Raulerson, E. K.; Li, X.; Goldzak, T.; Xia, P.; van Voorhis, T.; Tang, M. L.; Roberts, S. T. Surface States Mediate Triplet Energy Transfer in Nanocrystal-Acene Composite Systems. *J. Am. Chem. Soc.* **2018**, *140* (24), 7543−7553.
(75) Mahboub, M.; Huang, Z.; Tang, M. L. Efficient Infrared-to-Visible Upconversion with Subsolar Irradiance. *Nano Lett.* **2016**, *16* (11), 7169−7175.
(76) Huang, Z.; Li, X.; Mahboub, M.; Hanson, K. M.; Nichols, V. M.; Le, H.; Tang, M. L.; Bardeen, C. J. Hybrid Molecule-Nanocrystal Photon Upconversion across the Visible and near-Infrared. *Nano Lett.* **2015**, *15* (8), 5552−5557.
(77) Huang, Z.; Simpson, D. E.; Mahboub, M.; Li, X.; Tang, M. L. Ligand Enhanced Upconversion of Near-Infrared Photons with Nanocrystal Light Absorbers. *Chem. Sci.* **2016**, *7* (7), 4101−4104.
(78) Nishimura, N.; Allardice, J. R.; Xiao, J.; Gu, Q.; Gray, V.; Rao, A. Photon Upconversion Utilizing Energy beyond the Band Gap of Crystalline Silicon with a Hybrid TES-ADT/PbS Quantum Dots System. *Chem. Sci.* **2019**, *10* (18), 4750−4760.
(79) Protesescu, L.; Yakunin, S.; Bodnarchuk, M. I.; Krieg, F.; Caputo, R.; Hendon, C. H.; Yang, R. X.; Walsh, A.; Kovalenko, M. v. Nanocrystals of Cesium Lead Halide Perovskites (CsPbX3, X= Cl, Br, and I): Novel Optoelectronic Materials Showing Bright Emission with Wide Color Gamut. *Nano Lett.* **2015**, *15* (6), 3692−3696.
(80) Luo, X.; Liang, G.; Han, Y.; Li, Y.; Ding, T.; He, S.; Liu, X.; Wu, K. Triplet Energy Transfer from Perovskite Nanocrystals Mediated by Electron Transfer. *J. Am. Chem. Soc.* **2020**, *142* (25), 11270−11278.
(81) Mase, K.; Okumura, K.; Yanai, N.; Kimizuka, N. Triplet Sensitization by Perovskite Nanocrystals for Photon Upconversion. *Chem. Commun.* **2017**, *53* (59), 8261−8264.
(82) He, S.; Han, Y.; Guo, J.; Wu, K. Entropy-Gated Thermally Activated Delayed Emission Lifetime in Phenanthrene-Functionalized CsPbBr3 Perovskite Nanocrystals. *J. Phys. Chem. Lett.* **2021**, *12* (35), 8598−8604.
(83) Xie, R.; Rutherford, M.; Peng, X. Formation of High-Quality I-III-VI Semiconductor Nanocrystals by Tuning Relative Reactivity of Cationic Precursors. *J. Am. Chem. Soc.* **2009**, *131* (15), 5691−5697.
(84) Xia, C.; Wang, W.; Du, L.; Rabouw, F. T.; J. van den Heuvel, D.; Gerritsen, H. C.; Mattoussi, H.; de Mello Donega, C. Förster Resonance Energy Transfer between Colloidal CuInS2/ZnS Quantum Dots and Dark Quenchers. *J. Phys. Chem. C* **2020**, *124* (2), 1717−1731.
(85) Han, Y.; He, S.; Luo, X.; Li, Y.; Chen, Z.; Kang, W.; Wang, X.; Wu, K. Triplet Sensitization by "Self-Trapped" Excitons of Nontoxic CuInS2 Nanocrystals for Efficient Photon Upconversion. *J. Am. Chem. Soc.* **2019**, *141* (33), 13033−13037.
(86) Huang, C.-C.; Tang, Y.; van der Laan, M.; van de Groep, J.; Koenderink, A. F.; Dohnalová, K. Band-Gap Tunability in Partially Amorphous Silicon Nanoparticles Using Single-Dot Correlative Microscopy. *ACS Applied Nano Materials* **2021**, *4* (1), 288−296.
(87) Xia, P.; Raulerson, E. K.; Coleman, D.; Gerke, C. S.; Mangolini, L.; Tang, M. L.; Roberts, S. T. Achieving Spin-Triplet Exciton Transfer between Silicon and Molecular Acceptors for Photon Upconversion. *Nat. Chem.* **2020**, *12* (2), 137−144.
(88) Chen, G.; Damasco, J.; Qiu, H.; Shao, W.; Ohulchanskyy, T. Y.; Valiev, R. R.; Wu, X.; Han, G.; Wang, Y.; Yang, C.; Ågren, H.; Prasad, P. N. Energy-Cascaded Upconversion in an Organic Dye-Sensitized Core/Shell Fluoride Nanocrystal. *Nano Lett.* **2015**, *15* (11), 7400−7407.
(89) Law, M.; Luther, J. M.; Song, Q.; Hughes, B. K.; Perkins, C. L.; Nozik, A. J. Structural, Optical, and Electrical Properties of PbSe Nanocrystal Solids Treated Thermally or with Simple Amines. *J. Am. Chem. Soc.* **2008**, *130* (18), 5974−5985.
(90) Luther, J. M.; Law, M.; Song, Q.; Perkins, C. L.; Beard, M. C.; Nozik, A. J. Structural, Optical, and Electrical Properties of Self-Assembled Films of PbSe Nanocrystals Treated with 1,2-Ethanedithiol. *ACS Nano* **2008**, *2* (2), 271−280.
(91) Konstantatos, G.; Levina, L.; Tang, J.; Sargent, E. H. Sensitive Solution-Processed Bi2S3 Nanocrystalline Photodetectors. *Nano Lett.* **2008**, *8* (11), 4002−4006.
(92) Schlamp, M. C.; Peng, X.; Alivisatos, A. Improved Efficiencies in Light Emitting Diodes Made with CdSe (CdS) Core/Shell Type Nanocrystals and a Semiconducting Polymer. *J. Appl. Phys.* **1997**, *82* (11), 5837−5842.
(93) Talapin, D. v; Murray, C. B. PbSe Nanocrystal Solids for N-and p-Channel Thin Film Field-Effect Transistors. *Science (1979)* **2005**, *310* (5745), 86−89.
(94) Lingley, Z.; Lu, S.; Madhukar, A. The Dynamics of Energy and Charge Transfer in Lead Sulfide Quantum Dot Solids. *J. Appl. Phys.* **2014**, *115* (8), 084302.
(95) Zillner, E.; Fengler, S.; Niyamakom, P.; Rauscher, F.; Köhler, K.; Dittrich, T. Role of Ligand Exchange at CdSe Quantum Dot Layers for Charge Separation. *J. Phys. Chem. C* **2012**, *116* (31), 16747−16754.
(96) Fisher, A. A. E.; Osborne, M. A.; Day, I. J.; Alcalde, G. L. Measurement of Ligand Coverage on Cadmium Selenide Nanocryst-

als and Its Influence on Dielectric Dependent Photoluminescence Intermittency. *Commun. Chem.* **2019**, *2* (1), 63.
(97) Algar, W. R.; Krull, U. J. Multidentate Surface Ligand Exchange for the Immobilization of CdSe/ZnS Quantum Dots and Surface Quantum Dot-Oligonucleotide Conjugates. *Langmuir* **2008**, *24* (10), 5514−5520.
(98) Vickers, E. T.; Graham, T. A.; Chowdhury, A. H.; Bahrami, B.; Dreskin, B. W.; Lindley, S.; Naghadeh, S. B.; Qiao, Q.; Zhang, J. Z. Improving Charge Carrier Delocalization in Perovskite Quantum Dots by Surface Passivation with Conductive Aromatic Ligands. *ACS Energy Letters* **2018**, *3* (12), 2931−2939.
(99) Straus, D. B.; Goodwin, E. D.; Gaulding, E. A.; Muramoto, S.; Murray, C. B.; Kagan, C. R. Increased Carrier Mobility and Lifetime in CdSe Quantum Dot Thin Films through Surface Trap Passivation and Doping. *J. Phys. Chem. Lett.* **2015**, *6* (22), 4605−4609.
(100) Kirkwood, N.; Monchen, J. O. v; Crisp, R. W.; Grimaldi, G.; Bergstein, H. A. C.; du Fossé, I.; van der Stam, W.; Infante, I.; Houtepen, A. J. Finding and Fixing Traps in II-VI and III-V Colloidal Quantum Dots: The Importance of Z-Type Ligand Passivation. *J. Am. Chem. Soc.* **2018**, *140* (46), 15712−15723.
(101) Wang, L.; Lv, Y.; Lin, J.; Zhao, J.; Liu, X.; Zeng, R.; Wang, X.; Zou, B. Surface Organic Ligand-Passivated Quantum Dots: Toward High-Performance Light-Emitting Diodes with Long Lifetimes. *Journal of Materials Chemistry C* **2021**, *9* (7), 2483−2490.
(102) Hines, D. A.; Kamat, P. v. Recent Advances in Quantum Dot Surface Chemistry. *ACS Appl. Mater. Interfaces* **2014**, *6* (5), 3041−3057.
(103) Bera, D.; Qian, L.; Tseng, T.-K.; Holloway, P. H. Quantum Dots and Their Multimodal Applications: A Review. *Materials* **2010**, *3* (4), 2260−2345.
(104) Rossi, L. M.; Fiorio, J. L.; Garcia, M. A. S.; Ferraz, C. P. The Role and Fate of Capping Ligands in Colloidally Prepared Metal Nanoparticle Catalysts. *Dalton Transactions* **2018**, *47* (17), 5889−5915.
(105) de Roo, J.; Ibáñez, M.; Geiregat, P.; Nedelcu, G.; Walravens, W.; Maes, J.; Martins, J. C.; van Driessche, I.; Kovalenko, M. v; Hens, Z. Highly Dynamic Ligand Binding and Light Absorption Coefficient of Cesium Lead Bromide Perovskite Nanocrystals. *ACS Nano* **2016**, *10* (2), 2071−2081.
(106) Green, M. The Nature of Quantum Dot Capping Ligands. *J. Mater. Chem.* **2010**, *20* (28), 5797−5809.
(107) Lin, W.; Walter, J.; Burger, A.; Maid, H.; Hirsch, A.; Peukert, W.; Segets, D. A General Approach to Study the Thermodynamics of Ligand Adsorption to Colloidal Surfaces Demonstrated by Means of Catechols Binding to Zinc Oxide Quantum Dots. *Chem. Mater.* **2015**, *27* (1), 358−369.
(108) Bandyopadhyay, A.; Yamijala, S. S.; Pati, S. K. Tuning the Electronic and Optical Properties of Graphene and Boron-Nitride Quantum Dots by Molecular Charge-Transfer Interactions: A Theoretical Study. *Phys. Chem. Chem. Phys.* **2013**, *15* (33), 13881−13887.
(109) Zheng, X. T.; Ananthanarayanan, A.; Luo, K. Q.; Chen, P. Glowing Graphene Quantum Dots and Carbon Dots: Properties, Syntheses, and Biological Applications. *small* **2015**, *11* (14), 1620−1636.
(110) Zarghami, M. H.; Liu, Y.; Gibbs, M.; Gebremichael, E.; Webster, C.; Law, M. P-Type PbSe and PbS Quantum Dot Solids Prepared with Short-Chain Acids and Diacids. *ACS Nano* **2010**, *4* (4), 2475−2485.
(111) Bullen, C.; Mulvaney, P. The Effects of Chemisorption on the Luminescence of CdSe Quantum Dots. *Langmuir* **2006**, *22* (7), 3007−3013.
(112) Zhang, X.; Huang, H.; Maung, Y. M.; Yuan, J.; Ma, W. Aromatic Amine-Assisted Pseudo-Solution-Phase Ligand Exchange in CsPbI 3 Perovskite Quantum Dot Solar Cells. *Chem. Commun.* **2021**, *57* (64), 7906−7909.
(113) Munro, A. M.; Bardecker, J. A.; Liu, M. S.; Cheng, Y.-J.; Niu, Y.-H.; Jen-La Plante, I.; Jen, A. K.-Y.; Ginger, D. S. Colloidal CdSe Quantum Dot Electroluminescence: Ligands and Light-Emitting Diodes. *Microchimica Acta* **2008**, *160* (3), 345−350.
(114) Talapin, D. v; Rogach, A. L.; Mekis, I.; Haubold, S.; Kornowski, A.; Haase, M.; Weller, H. Synthesis and Surface Modification of Amino-Stabilized CdSe, CdTe and InP Nanocrystals. *Colloids Surf., A* **2002**, *202* (2−3), 145−154.
(115) Wang, Q.; Xu, Y.; Zhao, X.; Chang, Y.; Liu, Y.; Jiang, L.; Sharma, J.; Seo, D.-K.; Yan, H. A Facile One-Step in Situ Functionalization of Quantum Dots with Preserved Photoluminescence for Bioconjugation. *J. Am. Chem. Soc.* **2007**, *129* (20), 6380−6381.
(116) Lystrom, L.; Roberts, A.; Dandu, N.; Kilina, S. Surface-Induced Deprotonation of Thiol Ligands Impacts the Optical Response of CdS Quantum Dots. *Chem. Mater.* **2021**, *33* (3), 892−901.
(117) Bonilla, C. A. M.; Flórez, M.-H. T.; Velasco, D. R. M.; Kouznetsov, V. v. Surface Characterization of Thiol Ligands on CdTe Quantum Dots: Analysis by 1 H NMR and DOSY. *New J. Chem.* **2019**, *43* (22), 8452−8458.
(118) Morris-Cohen, A. J.; Donakowski, M. D.; Knowles, K. E.; Weiss, E. A. The Effect of a Common Purification Procedure on the Chemical Composition of the Surfaces of CdSe Quantum Dots Synthesized with Trioctylphosphine Oxide. *J. Phys. Chem. C* **2010**, *114* (2), 897−906.
(119) Morris-Cohen, A. J.; Frederick, M. T.; Lilly, G. D.; McArthur, E. A.; Weiss, E. A. Organic Surfactant-Controlled Composition of the Surfaces of CdSe Quantum Dots. *J. Phys. Chem. Lett.* **2010**, *1* (7), 1078−1081.
(120) Giovanelli, E.; Muro, E.; Sitbon, G.; Hanafi, M.; Pons, T.; Dubertret, B.; Lequeux, N. Highly Enhanced Affinity of Multidentate versus Bidentate Zwitterionic Ligands for Long-Term Quantum Dot Bioimaging. *Langmuir* **2012**, *28* (43), 15177−15184.
(121) Krieg, F.; Ochsenbein, S. T.; Yakunin, S.; ten Brinck, S.; Aellen, P.; Süess, A.; Clerc, B.; Guggisberg, D.; Nazarenko, O.; Shynkarenko, Y.; et al. Colloidal CsPbX3 (X= Cl, Br, I) Nanocrystals 2.0: Zwitterionic Capping Ligands for Improved Durability and Stability. *ACS Energy Lett.* **2018**, *3* (3), 641−646.
(122) Yuan, Y.; Zhu, H.; Hills-Kimball, K.; Cai, T.; Shi, W.; Wei, Z.; Yang, H.; Candler, Y.; Wang, P.; He, J.; Chen, O. Stereoselective C- C Oxidative Coupling Reactions Photocatalyzed by Zwitterionic Ligand Capped CsPbBr3 Perovskite Quantum Dots. *Angew. Chem., Int. Ed.* **2020**, *59* (50), 22563−22569.
(123) Wang, S.; Du, L.; Jin, Z.; Xin, Y.; Mattoussi, H. Enhanced Stabilization and Easy Phase Transfer of CsPbBr3 Perovskite Quantum Dots Promoted by High-Affinity Polyzwitterionic Ligands. *J. Am. Chem. Soc.* **2020**, *142* (29), 12669−12680.
(124) Wang, X.-S.; Dykstra, T. E.; Salvador, M. R.; Manners, I.; Scholes, G. D.; Winnik, M. A. Surface Passivation of Luminescent Colloidal Quantum Dots with Poly (Dimethylaminoethyl Methacrylate) through a Ligand Exchange Process. *J. Am. Chem. Soc.* **2004**, *126* (25), 7784−7785.
(125) Wang, M.; Dykstra, T. E.; Lou, X.; Salvador, M. R.; Scholes, G. D.; Winnik, M. A. Colloidal CdSe Nanocrystals Passivated by a Dye-Labeled Multidentate Polymer: Quantitative Analysis by Size-Exclusion Chromatography. *Angew. Chem., Int. Ed.* **2006**, *45* (14), 2221−2224.
(126) du Fossé, I.; Lal, S.; Hossaini, A. N.; Infante, I.; Houtepen, A. J. Effect of Ligands and Solvents on the Stability of Electron Charged CdSe Colloidal Quantum Dots. *J. Phys. Chem. C* **2021**, *125* (43), 23968−23975.
(127) Wong, M. W.; Wiberg, K. B.; Frisch, M. J. Solvent Effects. 3. Tautomeric Equilibria of Formamide and 2-Pyridone in the Gas Phase and Solution: An Ab Initio SCRF Study. *J. Am. Chem. Soc.* **1992**, *114* (5), 1645−1652.
(128) Huang, Z.; Xu, Z.; Huang, T.; Gray, V.; Moth-Poulsen, K.; Lian, T.; Tang, M. L. Evolution from Tunneling to Hopping Mediated Triplet Energy Transfer from Quantum Dots to Molecules. *J. Am. Chem. Soc.* **2020**, *142* (41), 17581−17588.

(129) Li, X.; Huang, Z.; Zavala, R.; Tang, M. L. Distance-Dependent Triplet Energy Transfer between CdSe Nanocrystals and Surface Bound Anthracene. *J. Phys. Chem. Lett.* **2016**, *7* (11), 1955−1959.
(130) Gray, V.; Zhang, Z.; Dowland, S.; Allardice, J. R.; Alvertis, A. M.; Xiao, J.; Greenham, N. C.; Anthony, J. E.; Rao, A. Thiol-Anchored TIPS-Tetracene Ligands with Quantitative Triplet Energy Transfer to PbS Quantum Dots and Improved Thermal Stability. *J. Phys. Chem. Lett.* **2020**, *11* (17), 7239−7244.
(131) Scholes, G. D. Long-Range Resonance Energy Transfer in Molecular Systems. *Annu. Rev. Phys. Chem.* **2003**, *54* (1), 57−87.
(132) Hofmann, C. C.; Bauer, P.; Haque, S. A.; Thelakkat, M.; Köhler, J. Energy-and Charge-Transfer Processes in Flexible Organic Donor-Acceptor Dyads. *J. Chem. Phys.* **2009**, *131* (14), 144512.
(133) Guo, Y.; Nehlmeier, I.; Poole, E.; Sakonsinsiri, C.; Hondow, N.; Brown, A.; Li, Q.; Li, S.; Whitworth, J.; Li, Z.; et al. Dissecting Multivalent Lectin-Carbohydrate Recognition Using Polyvalent Multifunctional Glycan-Quantum Dots. *J. Am. Chem. Soc.* **2017**, *139* (34), 11833−11844.
(134) Muller, P. Glossary of Terms Used in Physical Organic Chemistry (IUPAC Recommendations 1994). *Pure Appl. Chem.* **1994**, *66* (5), 1077−1184.
(135) Thompson, N. J.; Wilson, M. W. B.; Congreve, D. N.; Brown, P. R.; Scherer, J. M.; Bischof, T. S.; Wu, M.; Geva, N.; Welborn, M.; van Voorhis, T.; et al. Energy Harvesting of Non-Emissive Triplet Excitons in Tetracene by Emissive PbS Nanocrystals. *Nat. Mater.* **2014**, *13* (11), 1039−1043.
(136) Kim, E.; Park, S. B. Chemistry as a Prism: A Review of Light-Emitting Materials Having Tunable Emission Wavelengths. *Chemistry-An Asian Journal* **2009**, *4* (11), 1646−1658.
(137) Jones, G. A.; Bradshaw, D. S. Resonance Energy Transfer: From Fundamental Theory to Recent Applications. *Front. Phys.* **2019**, *7*, 100.
(138) Kuriakose, A. C.; Udayan, S.; Rose, T. P.; Nampoori, V. P. N.; Thomas, S. Synergistic Effects of CdS QDs-Neutral Red Dye Hybrid System on Its Nonlinear Optical Properties. *Opt. Laser Technol.* **2021**, *142*, 107261.
(139) Gopi, A.; Lingamoorthy, S.; Soman, S.; Yoosaf, K.; Haridas, R.; Das, S. Modulating FRET in Organic-Inorganic Nanohybrids for Light Harvesting Applications. *J. Phys. Chem. C* **2016**, *120* (46), 26569−26578.
(140) Cardoso Dos Santos, M.; Algar, W. R.; Medintz, I. L.; Hildebrandt, N. Hybrid. *TrAC Trends Anal. Chem.* **2020**, *125*, 115819.
(141) Roth, S.; Trinh, P. T.; Wachtveitl, J. Two-Photon Absorption Enhancement for Organic Acceptor Molecules with QD Antennas. *Nanoscale* **2021**, *13* (21), 9808−9815.
(142) Fernandez-Arguelles, M. T.; Yakovlev, A.; Sperling, R. A.; Luccardini, C.; Gaillard, S.; Sanz Medel, A.; Mallet, J.-M.; Brochon, J.-C.; Feltz, A.; Oheim, M.; Parak, W. J. Synthesis and Characterization of Polymer-Coated Quantum Dots with Integrated Acceptor Dyes as FRET-Based Nanoprobes. *Nano Lett.* **2007**, *7* (9), 2613−2617.
(143) Kotresh, M. G.; Adarsh, K. S.; Shivkumar, M. A.; Mulimani, B. G.; Savadatti, M. I.; Inamdar, S. R. Spectroscopic Investigation of Alloyed Quantum Dot-based FRET to Cresyl Violet Dye. *Luminescence* **2016**, *31* (3), 760−768.
(144) Michaelis, J.; van der Heden van Noort, G. J.; Seitz, O. DNA-Triggered Dye Transfer on a Quantum Dot. *Bioconjug Chem.* **2014**, *25* (1), 18−23.
(145) Jung, S.; Chen, X. Quantum Dot-Dye Conjugates for Biosensing, Imaging, and Therapy. *Adv. Healthc Mater.* **2018**, *7* (14), 1800252.
(146) Clapp, A. R.; Medintz, I. L.; Mauro, J. M.; Fisher, B. R.; Bawendi, M. G.; Mattoussi, H. Fluorescence Resonance Energy Transfer between Quantum Dot Donors and Dye-Labeled Protein Acceptors. *J. Am. Chem. Soc.* **2004**, *126* (1), 301−310.
(147) Kowerko, D.; Krause, S.; Amecke, N.; Abdel-Mottaleb, M.; Schuster, J.; von Borczyskowski, C. Identification of Different Donor-Acceptor Structures via Förster Resonance Energy Transfer (FRET) in Quantum-Dot-Perylene Bisimide Assemblies. *Int. J. Mol. Sci.* **2009**, *10* (12), 5239−5256.
(148) Chern, M.; Nguyen, T. T.; Mahler, A. H.; Dennis, A. M. Shell Thickness Effects on Quantum Dot Brightness and Energy Transfer. *Nanoscale* **2017**, *9* (42), 16446−16458.
(149) Díaz, S. A.; Lasarte Aragonés, G.; Buckhout-White, S.; Qiu, X.; Oh, E.; Susumu, K.; Melinger, J. S.; Huston, A. L.; Hildebrandt, N.; Medintz, I. L. Bridging Lanthanide to Quantum Dot Energy Transfer with a Short-Lifetime Organic Dye. *J. Phys. Chem. Lett.* **2017**, *8* (10), 2182−2188.
(150) Zhou, D.; Piper, J. D.; Abell, C.; Klenerman, D.; Kang, D.-J.; Ying, L. Fluorescence Resonance Energy Transfer between a Quantum Dot Donor and a Dye Acceptor Attached to DNA. *Chem. Commun.* **2005**, *38*, 4807−4809.
(151) Samanta, A.; Buckhout-White, S.; Oh, E.; Susumu, K.; Medintz, I. L. Exploring Attachment Chemistry with FRET in Hybrid Quantum Dot Dye-Labeled DNA Dendrimer Composites. *Molecular Systems Design & Engineering* **2018**, *3* (2), 314−327.
(152) Onoshima, D.; Kaji, N.; Tokeshi, M.; Baba, Y. Nuclease Tolerant FRET Probe Based on DNA-Quantum Dot Conjugation. *Anal. Sci.* **2008**, *24* (2), 181−183.
(153) Shivkumar, M. A.; Adarsh, K. S.; Inamdar, S. R. Quantum Dot Based FRET to Cresyl Violet: Role of Surface Effects. *J. Lumin.* **2013**, *143*, 680−686.
(154) Dworak, L.; Reuss, A. J.; Zastrow, M.; Rück-Braun, K.; Wachtveitl, J. Discrimination between FRET and Non-FRET Quenching in a Photochromic CdSe Quantum Dot/Dithienylethene Dye System. *Nanoscale* **2014**, *6* (23), 14200−14203.
(155) Xu, C. S.; Kim, H.; Yang, H.; Hayden, C. C. Multiparameter Fluorescence Spectroscopy of Single Quantum Dot- Dye FRET Hybrids. *J. Am. Chem. Soc.* **2007**, *129* (36), 11008−11009.
(156) Medintz, I. L.; Mattoussi, H. Quantum Dot-Based Resonance Energy Transfer and Its Growing Application in Biology. *Phys. Chem. Chem. Phys.* **2009**, *11* (1), 17−45.
(157) Suzuki, M.; Husimi, Y.; Komatsu, H.; Suzuki, K.; Douglas, K. T. Quantum Dot FRET Biosensors That Respond to PH, to Proteolytic or Nucleolytic Cleavage, to DNA Synthesis, or to a Multiplexing Combination. *J. Am. Chem. Soc.* **2008**, *130* (17), 5720−5725.
(158) Kuznetsova, V.; Tkach, A.; Cherevkov, S.; Sokolova, A.; Gromova, Y.; Osipova, V.; Baranov, M.; Ugolkov, V.; Fedorov, A.; Baranov, A. Spectral-Time Multiplexing in FRET Complexes of AgInS2/ZnS Quantum Dot and Organic Dyes. *Nanomaterials* **2020**, *10* (8), 1569.
(159) Conroy, E. M.; Li, J. J.; Kim, H.; Algar, W. R. Self-Quenching, Dimerization, and Homo-FRET in Hetero-FRET Assemblies with Quantum Dot Donors and Multiple Dye Acceptors. *J. Phys. Chem. C* **2016**, *120* (31), 17817−17828.
(160) Zhang, H.; Zhou, D. A Quantum Dot-Intercalating Dye Dual-Donor FRET Based Biosensor. *Chem. Commun.* **2012**, *48* (42), 5097−5099.
(161) Chi, C.-W.; Lao, Y.-H.; Li, Y.-S.; Chen, L.-C. A Quantum Dot-Aptamer Beacon Using a DNA Intercalating Dye as the FRET Reporter: Application to Label-Free Thrombin Detection. *Biosens. Bioelectron.* **2011**, *26* (7), 3346−3352.
(162) Medintz, I. L.; Clapp, A. R.; Mattoussi, H.; Goldman, E. R.; Fisher, B.; Mauro, J. M. Self-Assembled Nanoscale Biosensors Based on Quantum Dot FRET Donors. *Nat. Mater.* **2003**, *2* (9), 630−638.
(163) Halpert, J. E.; Tischler, J. R.; Nair, G.; Walker, B. J.; Liu, W.; Bulović, V.; Bawendi, M. G. Electrostatic Formation of Quantum Dot/J-Aggregate FRET Pairs in Solution. *J. Phys. Chem. C* **2009**, *113* (23), 9986−9992.
(164) Lim, T. C.; Bailey, V. J.; Ho, Y.-P.; Wang, T.-H. Intercalating Dye as an Acceptor in Quantum-Dot-Mediated FRET. *Nanotechnology* **2008**, *19* (7), 075701.
(165) Clapp, A. R.; Medintz, I. L.; Mattoussi, H. Förster Resonance Energy Transfer Investigations Using Quantum-dot Fluorophores. *ChemPhysChem* **2006**, *7* (1), 47−57.
(166) Dexter, D. L. A Theory of Sensitized Luminescence in Solids. *J. Chem. Phys.* **1953**, *21* (5), 836−850.

https://doi.org/10.1021/acsphyschemau.2c00018
ACS Phys. Chem Au 2022, 2, 364−387

(167) Köhler, A.; Bässler, H. What Controls Triplet Exciton Transfer in Organic Semiconductors? *J. Mater. Chem.* **2011**, *21* (12), 4003−4011.
(168) Tabachnyk, M.; Ehrler, B.; Gélinas, S.; Böhm, M. L.; Walker, B. J.; Musselman, K. P.; Greenham, N. C.; Friend, R. H.; Rao, A. Resonant Energy Transfer of Triplet Excitons from Pentacene to PbSe Nanocrystals. *Nat. Mater.* **2014**, *13* (11), 1033−1038.
(169) Lakowicz, J. R. *Principles of Fluorescence Spectroscopy*; Springer Science & Business Media, 2013.
(170) Walker, B. J.; Nair, G. P.; Marshall, L. F.; Bulović, V.; Bawendi, M. G. Narrow-Band Absorption-Enhanced Quantum Dot/J-Aggregate Conjugates. *J. Am. Chem. Soc.* **2009**, *131* (28), 9624−9625.
(171) Czikkely, V.; Försterling, H. D.; Kuhn, H. Light Absorption and Structure of Aggregates of Dye Molecules. *Chem. Phys. Lett.* **1970**, *6* (1), 11−14.
(172) Eisfeld, A.; Briggs, J. S. The J-and H-Bands of Organic Dye Aggregates. *Chem. Phys.* **2006**, *324* (2−3), 376−384.
(173) Nüesch, F.; Grätzel, M. H-Aggregation and Correlated Absorption and Emission of a Merocyanine Dye in Solution, at the Surface and in the Solid State. A Link between Crystal Structure and Photophysical Properties. *Chem. Phys.* **1995**, *193* (1−2), 1−17.
(174) Sheppard, S. E. The Effects of Environment and Aggregation on the Absorption Spectra of Dyes. *Rev. Mod. Phys.* **1942**, *14* (2−3), 303.
(175) Hens, Z.; Martins, J. C. A Solution NMR Toolbox for Characterizing the Surface Chemistry of Colloidal Nanocrystals. *Chem. Mater.* **2013**, *25* (8), 1211−1221.
(176) Arjona-Esteban, A.; Stolte, M.; Würthner, F. Conformational Switching of Π-Conjugated Junctions from Merocyanine to Cyanine States by Solvent Polarity. *Angew. Chem.* **2016**, *128* (7), 2516−2519.
(177) Hoche, J.; Schulz, A.; Dietrich, L. M.; Humeniuk, A.; Stolte, M.; Schmidt, D.; Brixner, T.; Würthner, F.; Mitric, R. The Origin of the Solvent Dependence of Fluorescence Quantum Yields in Dipolar Merocyanine Dyes. *Chem. Sci.* **2019**, *10* (48), 11013−11022.
(178) Dmitrenko, O. G.; Terenetskaya, I. P.; Reischl, W. Solvent Effect on Previtamin D Conformational Equilibrium and Photoreactions. *J. Photochem. Photobiol., A* **1997**, *104* (1−3), 113−117.
(179) Klymchenko, A. S.; Pivovarenko, V. G.; Demchenko, A. P. Perturbation of Planarity as the Possible Mechanism of Solvent-Dependent Variations of Fluorescence Quantum Yield in 2-Aryl-3-Hydroxychromones. *Spectrochimica Acta Part A: Molecular and Biomolecular Spectroscopy* **2003**, *59* (4), 787−792.
(180) Yang, W.; Yang, Y.; Kaledin, A. L.; He, S.; Jin, T.; McBride, J. R.; Lian, T. Surface Passivation Extends Single and Biexciton Lifetimes of InP Quantum Dots. *Chemical Science* **2020**, *11* (22), 5779−5789.
(181) Coughlan, C.; Ibáñez, M.; Dobrozhan, O.; Singh, A.; Cabot, A.; Ryan, K. M. Compound Copper Chalcogenide Nanocrystals. *Chem. Rev.* **2017**, *117* (9), 5865−6109.
(182) Kolny-Olesiak, J.; Weller, H. Synthesis and Application of Colloidal CuInS2 Semiconductor Nanocrystals. *ACS Appl. Mater. Interfaces* **2013**, *5* (23), 12221−12237.
(183) Knowles, K. E.; Hartstein, K. H.; Kilburn, T. B.; Marchioro, A.; Nelson, H. D.; Whitham, P. J.; Gamelin, D. R. Luminescent Colloidal Semiconductor Nanocrystals Containing Copper: Synthesis, Photophysics, and Applications. *Chem. Rev.* **2016**, *116* (18), 10820−10851.
(184) Xu, G.; Zeng, S.; Zhang, B.; Swihart, M. T.; Yong, K.-T.; Prasad, P. N. New Generation Cadmium-Free Quantum Dots for Biophotonics and Nanomedicine. *Chem. Rev.* **2016**, *116* (19), 12234−12327.
(185) Zou, W.; Li, L.; Chen, Y.; Chen, T.; Yang, Z.; Wang, J.; Liu, D.; Lin, G.; Wang, X. In Vivo Toxicity Evaluation of PEGylated CuInS(2)/ZnS Quantum Dots in BALB/c Mice. *Front Pharmacol* **2019**, *10*, 437.
(186) Ren, T.; Mandal, P. K.; Erker, W.; Liu, Z.; Avlasevich, Y.; Puhl, L.; Müllen, K.; Basché, T. A Simple and Versatile Route to Stable Quantum Dot-Dye Hybrids in Nonaqueous and Aqueous Solutions. *J. Am. Chem. Soc.* **2008**, *130* (51), 17242−17243.
(187) Smith, M. B.; Michl, J. Singlet Fission. *Chem. Rev.* **2010**, *110* (11), 6891−6936.
(188) Rao, A.; Friend, R. H. Harnessing Singlet Exciton Fission to Break the Shockley-Queisser Limit. *Nat. Rev. Mater.* **2017**, *2* (11), 17063.
(189) Scholes, G. D.; Rumbles, G. Excitons in Nanoscale Systems. *Nat. Mater.* **2006**, *5*, 683−696.
(190) Gray, V.; Allardice, J. R.; Zhang, Z.; Dowland, S.; Xiao, J.; Petty, A. J.; Anthony, J. E.; Greenham, N. C.; Rao, A. Direct vs Delayed Triplet Energy Transfer from Organic Semiconductors to Quantum Dots and Implications for Luminescent Harvesting of Triplet Excitons. *ACS Nano* **2020**, *14* (4), 4224−4234.
(191) Bossanyi, D. G.; Matthiesen, M.; Wang, S.; Smith, J. A.; Kilbride, R. C.; Shipp, J. D.; Chekulaev, D.; Holland, E.; Anthony, J. E.; Zaumseil, J.; Musser, A. J.; Clark, J. Emissive Spin-0 Triplet-Pairs Are a Direct Product of Triplet-Triplet Annihilation in Pentacene Single Crystals and Anthradithiophene Films. *Nature Chemistry 2020 13:2* **2021**, *13* (2), 163−171.
(192) Lindon, J. C., Koppenaal, D. W., Tranter, G. E., Eds. *Encyclopedia of Spectroscopy and Spectrometry*, 3rd ed.; Academic Press 2017.
(193) Garakyaraghi, S.; Castellano, F. N. Nanocrystals for Triplet Sensitization: Molecular Behavior from Quantum-Confined Materials. *Inorg. Chem.* **2018**, *57* (5), 2351−2359.
(194) Scholes, G. D. Controlling the Optical Properties of Inorganic Nanoparticles. *Adv. Funct. Mater.* **2008**, *18* (8), 1157−1172.
(195) Nienhaus, L.; Wu, M.; Bulović, V.; Baldo, M. A.; Bawendi, M. G. Using Lead Chalcogenide Nanocrystals as Spin Mixers: A Perspective on near-Infrared-to-Visible Upconversion. *Dalton Transactions* **2018**, *47* (26), 8509−8516.
(196) Murray, C. B.; Norris, D. J.; Bawendi, M. G. Synthesis and Characterization of Nearly Monodisperse CdE (E = Sulfur, Selenium, Tellurium) Semiconductor Nanocrystallites. *J. Am. Chem. Soc.* **1993**, *115* (19), 8706−8715.
(197) Efros, A. L.; Rosen, M.; Kuno, M.; Nirmal, M.; Norris, D.; Bawendi, M. Band-Edge Exciton in Quantum Dots of Semiconductors with a Degenerate Valence Band: Dark and Bright Exciton States. *Physical Review B - Condensed Matter and Materials Physics* **1996**, *54* (7), 4843−4856.
(198) Huang, Z.; Xu, Z.; Mahboub, M.; Li, X.; Taylor, J. W.; Harman, W. H.; Lian, T.; Tang, M. L. PbS/CdS Core-Shell Quantum Dots Suppress Charge Transfer and Enhance Triplet Transfer. *Angew. Chem.* **2017**, *129* (52), 16810−16814.
(199) Mongin, C.; Garakyaraghi, S.; Razgoniaeva, N.; Zamkov, M.; Castellano, F. N. Direct Observation of Triplet Energy Transfer from Semiconductor Nanocrystals. *Science (1979)* **2016**, *351* (6271), 369−372.
(200) Huang, Z.; Xu, Z.; Mahboub, M.; Liang, Z.; Jaimes, P.; Xia, P.; Graham, K. R.; Tang, M. L.; Lian, T. Enhanced Near-Infrared-to-Visible Upconversion by Synthetic Control of PbS Nanocrystal Triplet Photosensitizers. *J. Am. Chem. Soc.* **2019**, *141* (25), 9769−9772.
(201) Zhou, Y.; Castellano, F. N.; Schmidt, T. W.; Hanson, K. On the Quantum Yield of Photon Upconversion via Triplet-Triplet Annihilation. *ACS Energy Letters* **2020**, *5* (7), 2322−2326.
(202) Gray, V.; Xia, P.; Huang, Z.; Moses, E.; Fast, A.; Fishman, D. A.; Vullev, V. I.; Abrahamsson, M.; Moth-Poulsen, K.; Tang, M. L. CdS/ZnS Core-Shell Nanocrystal Photosensitizers for Visible to UV Upconversion. *Chem. Sci.* **2017**, *8* (8), 5488−5496.
(203) Singh-Rachford, T. N.; Castellano, F. N. Low Power Visible-to-UV Upconversion. *J. Phys. Chem. A* **2009**, *113* (20), 5912−5917.
(204) Verlman, I. B. *Handbook of Fluorescence Spectra of Aromatic Molecules*, 1st ed.; Academic Press, 1965.
(205) Ma, L.; Zhang, K.; Kloc, C.; Sun, H.; Michel-Beyerle, M. E.; Gurzadyan, G. G. Singlet Fission in Rubrene Single Crystal: Direct Observation by Femtosecond Pump-Probe Spectroscopy. *Phys. Chem. Chem. Phys.* **2012**, *14* (23), 8307−8312.
(206) Zhu, H.; Song, N.; Lian, T. Controlling Charge Separation and Recombination Rates in CdSe/ZnS Type I Core-Shell Quantum

Dots by Shell Thicknesses. *J. Am. Chem. Soc.* **2010**, *132* (42), 15038−15045.
(207) De Roo, J.; Huang, Z.; Schuster, N. J.; Hamachi, L. S.; Congreve, D. N.; Xu, Z.; Xia, P.; Fishman, D. A.; Lian, T.; Owen, J. S.; Tang, M. L. Anthracene Diphosphate Ligands for CdSe Quantum Dots; Molecular Design for Efficient Upconversion. *Chem. Mater.* **2020**, *32* (4), 1461−1466.
(208) Yang, Y.; Li, J.; Lin, L.; Peng, X. An Efficient and Surface-Benign Purification Scheme for Colloidal Nanocrystals Based on Quantitative Assessment. *Nano Research* **2015**, *8* (10), 3353−3364.
(209) Luo, X.; Lai, R.; Li, Y.; Han, Y.; Liang, G.; Liu, X.; Ding, T.; Wang, J.; Wu, K. Triplet Energy Transfer from CsPbBr3 Nanocrystals Enabled by Quantum Confinement. *J. Am. Chem. Soc.* **2019**, *141* (10), 4186−4190.
(210) Mahboub, M.; Maghsoudiganjeh, H.; Pham, A. M.; Huang, Z.; Tang, M. L. Triplet Energy Transfer from PbS(Se) Nanocrystals to Rubrene: The Relationship between the Upconversion Quantum Yield and Size. *Adv. Funct. Mater.* **2016**, *26* (33), 6091−6097.
(211) Huang, Z.; Li, X.; Yip, B. D.; Rubalcava, J. M.; Bardeen, C. J.; Tang, M. L. Nanocrystal Size and Quantum Yield in the Upconversion of Green to Violet Light with CdSe and Anthracene Derivatives. *Chem. Mater.* **2015**, *27* (21), 7503−7507.
(212) Koolyk, M.; Amgar, D.; Aharon, S.; Etgar, L. Kinetics of Cesium Lead Halide Perovskite Nanoparticle Growth; Focusing and de-Focusing of Size Distribution. *Nanoscale* **2016**, *8* (12), 6403−6409.
(213) Xia, P.; Schwan, J.; Dugger, T. W.; Mangolini, L.; Tang, M. L. Air-Stable Silicon Nanocrystal-Based Photon Upconversion. *Adv. Opt. Mater.* **2021**, *9* (17), 2100453.
(214) Vanorman, Z. A.; Bieber, A. S.; Wieghold, S.; Nienhaus, L. Green-to-Blue Triplet Fusion Upconversion Sensitized by Anisotropic CdSe Nanoplatelets. *Chem. Mater.* **2020**, *32* (11), 4734−4742.
(215) Vanorman, Z. A.; Conti, C. R.; Strouse, G. F.; Nienhaus, L. Red-to-Blue Photon Upconversion Enabled by One-Dimensional CdTe Nanorods. *Chem. Mater.* **2021**, *33* (1), 452−458.
(216) Shockley, W.; Queisser, H. J. Detailed Balance Limit of Efficiency of P-n Junction Solar Cells. *J. Appl. Phys.* **1961**, *32* (3), 510−519.
(217) Goldschmidt, J. C.; Fischer, S. Upconversion for Photovoltaics - a Review of Materials, Devices and Concepts for Performance Enhancement. *Advanced Optical Materials* **2015**, *3* (4), 510−535.
(218) Justo, Y.; Geiregat, P.; van Hoecke, K.; Vanhaecke, F.; De Mello Donega, C.; Hens, Z. Optical Properties of PbS/CdS Core/Shell Quantum Dots. *J. Phys. Chem. C* **2013**, *117* (39), 20171−20177.
(219) Parker, C. A.; Hatchard, C. G. Triplet-Singlet Emission in Fluid Solutions. Phosphorescence of Eosin. *Trans. Faraday Soc.* **1961**, *57* (0), 1894−1904.
(220) Maciejewski, A.; Szymanski, M.; Steer, R. P. Thermally Activated Delayed S1 Fluorescence of Aromatic Thiones. *J. Phys. Chem.* **1986**, *90* (23), 6314−6318.
(221) Olaru, M.; Rychagova, E.; Ketkov, S.; Shynkarenko, Y.; Yakunin, S.; Kovalenko, M. v.; Yablonskiy, A.; Andreev, B.; Kleemiss, F.; Beckmann, J.; Vogt, M. A Small Cationic Organo-Copper Cluster as Thermally Robust Highly Photo- And Electroluminescent Material. *J. Am. Chem. Soc.* **2020**, *142* (1), 373−381.
(222) Kaur, G.; Kaur, H.; Tripathi, S. K. *Fluorescence Relaxation Dynamics of CdSe and CdSe/CdS Core/Shell Quantum Dots ARTICLES YOU MAY BE INTERESTED IN* **2013**, *1591*, 420.
(223) Yonemoto, D. T.; Papa, C. M.; Sheykhi, S.; Castellano, F. N. Controlling Thermally Activated Delayed Photoluminescence in CdSe Quantum Dots through Triplet Acceptor Surface Coverage. *J. Phys. Chem. Lett.* **2021**, *12* (15), 3718−3723.
(224) Schmidt, T. W.; Castellano, F. N. Photochemical Upconversion: The Primacy of Kinetics. *J. Phys. Chem. Lett.* **2014**, *5* (22), 4062−4072.
(225) Di, D.; Yang, L.; Richter, J. M.; Meraldi, L.; Altamimi, R. M.; Alyamani, A. Y.; Credgington, D.; Musselman, K. P.; MacManus-Driscoll, J. L.; Friend, R. H. Efficient Triplet Exciton Fusion in Molecularly Doped Polymer Light-emitting Diodes. *Adv. Mater.* **2017**, *29* (13), 1605987.
(226) H. Sargent, E. Infrared Quantum Dots. *Adv. Mater.* **2005**, *17* (5), 515−522.
(227) Talapin, D. v; Lee, J.-S.; Kovalenko, M. v; Shevchenko, E. v. Prospects of Colloidal Nanocrystals for Electronic and Optoelectronic Applications. *Chem. Rev.* **2010**, *110* (1), 389−458.
(228) Neo, D. C. J.; Cheng, C.; Stranks, S. D.; Fairclough, S. M.; Kim, J. S.; Kirkland, A. I.; Smith, J. M.; Snaith, H. J.; Assender, H. E.; Watt, A. A. R. Influence of Shell Thickness and Surface Passivation on PbS/CdS Core/Shell Colloidal Quantum Dot Solar Cells. *Chem. Mater.* **2014**, *26* (13), 4004−4013.
(229) Shirasaki, Y.; Supran, G. J.; Bawendi, M. G.; Bulović, V. Emergence of Colloidal Quantum-Dot Light-Emitting Technologies. *Nat. Photonics* **2013**, *7* (1), 13−23.

https://doi.org/10.1021/acsphyschemau.2c00018
ACS Phys. Chem Au 2022, 2, 364−387